A Novel Chronic *in vivo* Oral Cadmium Exposure-Washout Mouse Model for Studying Cadmium Toxicity and Complex Diabetogenic Effects

Winifred P.S. Wong[1], Janice C. Wang[1], Matthew S. Meyers[1], Nathan J. Wang[1], Rebecca A. Sponenburg[2], Norrina B. Allen[3], Joshua E. Edwards[4], Malek El Muayed[1*]

[1]Division of Endocrinology, Metabolism and Molecular Medicine, Feinberg School of Medicine, Northwestern University, Chicago, IL 60611, USA.

[2]Quantitative Bio-element Imaging Centre, Chemistry of Life Processes, Northwestern University, Evanston, IL 60208, USA.

[3]Institute for Public Health and Medicine, Center for Epidemiology and Population Health, Feinberg School of Medicine, Northwestern University, Chicago, IL 60611, USA.

[4]College of Graduate Studies, Midwestern University, Downers Grove, IL 60515, USA.

*Corresponding author: Email: m-muayed@northwestern.edu

Abstract

Type II diabetes mellitus (T2DM) is characterized by insulin resistance, β-cell dysfunction and hyperglycemia. In addition to well known risk factors such as lifestyle and genetic risk score, accumulation of environmental toxicants in organs relevant to glucose metabolism is increasingly recognized as additional risk factors for T2DM. Here, we describe the development of an *in vivo* oral cadmium (Cd) exposure model. It was shown that oral Cd exposure in drinking water followed by washout and high fat diet (HFD) in C57BL/6N mice results in islet Cd bioaccumulation comparable to that found in native human islets while mitigating the anorexic effects of Cd to achieve the same weight gain required to induce insulin resistance as in Cd naïve control mice. Inter individual variation in plasma glucose and insulin levels as well as islet Cd bioaccumulation was observed in both female and male mice. Regression analysis showed an inverse correlation between islet Cd level and plasma insulin following a glucose challenge in males but not in females. This finding highlights the need to account for inter individual target tissue Cd concentrations when interpreting results from *in vivo* Cd exposure models. No effect of Cd on insulin secretion was observed in islets *ex vivo*, highlighting differences between *in vivo* and *ex vivo* cadmium exposure models. In summary, our oral *in vivo* Cd exposure-washout with HFD model resulted in islet Cd bioaccumulation that is relevant in the context of environmental cadmium exposure in humans. Here, we showed that islet Cd bioaccumulation is associated with complex cadmium-mediated changes in glucose clearance and β-cell function. The model described here will serve as a useful tool to further examine the relationship between Cd exposure, islet Cd bioaccumulation, dysglycemia and their underlying mechanisms.

Introduction

Type II diabetes mellitus (T2DM) is characterized by insulin resistance and dysfunction of insulin-secreting β-cells within pancreatic islets of Langerhans (Petersmann, Muller-Wieland et al. 2019). The development of T2DM is dependent upon the interplay of many factors. Several genetic variations (Todd, Srinivasan et al. 2018, Banerjee, Vats et al. 2019), intrauterine environment (Fernandez-Twinn, Hjort et al. 2019) and lifestyle-related factors including obesity, diet, physical inactivity and smoking have been associated with susceptibility of T2DM (Kolb and Martin 2017). In addition to these risk factors, increasing evidence suggests that exposure to environmental toxicants such as arsenic (Martin, Gonzalez-Horta et al. 2015, Kuo, Moon et al. 2017, Beck, Chandi et al. 2019, Li, Douillet et al. 2020) and cadmium (Cd) (Schwartz, Il'yasova et al. 2003) as contributors to the development of T2DM.

To date, studies in humans and animal models describing the relationship between Cd exposure on diabetes are inconsistent. Some epidemiologic studies showed an association between Cd exposure and impaired glucose homeostasis (Bell, Early et al. 1990, Schwartz, Il'yasova et al. 2003, Afridi, Kazi et al. 2008, Fitzgerald, Olsen et al. 2020) while others reported the lack of an association (Barregard, Bergstrom et al. 2013, Menke, Guallar et al. 2016). Cadmium is a transition metal with toxic properties that is found at low levels in fruits, grains and vegetables grown on Cd-containing soil (Jolly, Islam et al. 2013), drinking water (Dalmieda and Kruse 2019) and cigarette smoke (Scherer and Barkemeyer 1983). Exposure to environmental cadmium through ingestion of Cd-containing food components and inhalation of cigarette smoke results in gradual

62 accumulation of Cd in various organs including insulin-producing pancreatic islets (Wong,
63 Allen et al. 2017). In mice, short term Cd exposure *in vivo* given as subcutaneous
64 injections resulted in bioaccumulation of Cd in pancreatic islets and dysglycemia
65 (Fitzgerald, Olsen et al. 2020). In dispersed mouse islet cell culture, bioaccumulation of
66 intracellular Cd was associated with a blunted glucose-stimulated insulin secretion (El
67 Muayed, Raja et al. 2012). Further studies examining the effects and mechanisms of
68 sustained, oral Cd in insulin-producing islets at environmentally relevant concentrations
69 while avoiding acute systemic toxicity are warranted. Cadmium has a long tissue half-life
70 of up to 30 years and thus, results in gradual Cd accumulation in human tissues over
71 decades (Elinder, Lind et al. 1976, Jarup and Akesson 2009) with the highest levels in
72 the kidney cortex reached at age 50 (Friberg 1984). Replicating similar rates of tissue Cd
73 accumulation in a murine model is of high importance for examining the effect of Cd at
74 tissue levels but at the same time, poses unique challenges relating to the long half-life
75 of Cd and its low oral bioavailability of 2-4% (Schilderman, Moonen et al. 1997).
76
77 In the present study, we established a novel *in vivo* oral Cd exposure murine model with
78 an initial oral Cd exposure phase followed by a washout phase with high fat feeding aimed
79 at replicating chronic islet Cd accumulation in the setting of insulin resistance in humans
80 over a reasonable time frame. Our Cd exposure-washout with high fat feeding mouse
81 model results in near baseline systemic Cd levels while achieving islet Cd
82 bioaccumulation that are within range of those found in native human islets from the
83 general population (Wong, Allen et al. 2017). We used this model to investigate the

84 effects of Cd bioaccumulation in pancreatic islets on β-cell function at islet Cd
85 concentrations that are relevant to human environmental Cd exposure.
86
87 **Material and methods**
88 **Cadmium exposure in mice**
89 5-6 weeks old, C57BL/6N mice were exposed to either vehicle or 0.5mM (=56.2ppm Cd,
90 56.2 mg/L Cd) or 1mM $CdCl_2$ (112.4ppm Cd, 112.4 mg/L Cd) (Rigaku, Cat #: 1008154)
91 in deionized drinking water (18.2μΩ, Millipore) acidified with HCl (30μM, Fisher Scientific)
92 for varying duration as indicated. During Cd exposure, mice were fed regular chow
93 (Envigo, Cat #: 7912) *ad libitum* unless otherwise stated. Experiments were carried out
94 in several successive cohorts designed to test the effect of various exposure parameters
95 as detailed in Table 1. In some experiments, mice were transitioned from $CdCl_2$-
96 containing drinking water to vehicle drinking water during a subsequent washout phase.
97 Mice were fed either regular chow (Envigo, Cat #: 7912) or adjusted calories high fat
98 rodent chow (Envigo, Cat #: TD88137, TD180240, 42% from fat) *ad libitum* during the
99 exposure and/or washout phase as described. Drinking water was changed once a week
100 to ensure freshness throughout all experimental phases. Metal analysis of regular and
101 high fat chow used are summarized in Suppl. Table 3. At the conclusion of the study,
102 mice were euthanized and tissues were collected for further analysis. All animal
103 experiments were reviewed and approved by the Institutional Animal Care and Use
104 Committee of Northwestern University.
105
106 ***In vivo* glucose tolerance tests and glucose-stimulated insulin secretion**

107 Standard glucose tolerance test (GTT) was performed by injecting a glucose bolus (50%
108 dextrose, pH 4.2, Hospira, Cat #: 000622) into the intraperitoneal cavity at a dose of 1g/kg
109 body weight following an overnight fast of 16-18 hours (Ayala, Samuel et al. 2010). Blood
110 was drawn through a tail capillary before glucose injection (t=0 min) and at 2, 5, 15, 30,
111 60 and 120 minutes post-glucose load for blood glucose determination. *In vivo* glucose-
112 stimulated insulin secretion (GSIS) was performed using a higher glucose dose of 3g/kg
113 body weight (Ayala, Samuel et al. 2010). Blood sampling time points from tail capillary
114 for glucose measurements during GSIS were similar to that of GTT tests. Blood glucose
115 concentrations were measured using an Accu-Chek Nano glucose meter (Roche
116 Diagnostics). For GSIS, 20μl of blood was also collected and separated in heparinized
117 microvette tubes (Sarstedt, Germany, Cat #: CB300LH) before glucose injection (t=0min)
118 and at 2, 5, 15 and 30 minutes post-glucose load for plasma insulin analysis. Plasma
119 samples were stored at -80°C until measurements of plasma insulin that was performed
120 using ELISA kits (Crystal Chem, Cat #: 90080). In some experiments, additional plasma
121 samples were obtained for determination of proinsulin levels (Mercodia, Cat #: 10-1232-
122 01).
123
124 **Hyperglycemic clamp**
125 Hyperglycemic clamps were performed by the Mouse Metabolic Phenotyping Center
126 (MMPC), Vanderbilt University, Tennessee. Briefly, 5 days prior to clamp studies,
127 catheters were implanted into the carotid artery and jugular veins for sampling and
128 infusion respectively. Hyperglycemic clamps were performed in unrestrained, conscious
129 mice following 5 hours fast (Ayala, Samuel et al. 2010). At t=0 min, blood glucose was

130 raised and continuous glucose infusion rate adjusted to maintain hyperglycemic plateau
131 between 250-300mg/dl (13.8-16.7mM) based on arterial blood glucose measurements at
132 10 min intervals. Mice received heparinized saline- washed mouse erythrocytes from
133 donors at 5μl/min to prevent a drop in hematocrit. Baseline arterial blood glucose, insulin
134 and c-peptide were measured at -15 and -5 minutes prior to clamp. Arterial blood
135 sampling for clamp insulin was measured at 5, 10, 15, 20, 40, 60, 80, 100 and 120 minutes
136 during clamp. Arterial c-peptide was measured at 15, 100 and 120 minutes during clamp.
137 Plasma insulin and plasma c-peptide were measured using radioimmunoassay (EMD
138 Sigma, Cat #: RI-13K) and bead immunoassay (Luminex, R&D Systems) respectively that
139 were used according to manufacturer's instructions. Following completion of clamp
140 studies, mice were returned to regular housing for at least 48 hours with food and water
141 available *ad libitum* prior to islet perifusion studies.
142
143 **Pancreatic islet isolation**
144 Islet isolation was performed as previously described (El-Muayed, Raja et al. 2012). In
145 brief, C57BL/6N mice were anaesthetized with intraperitoneal injection of ketamine
146 (10mg/ml)/xylazine (1mg/ml) and the abdominal cavity opened to expose the common
147 bile duct. Pancreas was perfused with 3ml collagenase (0.5mg/ml, Sigma, Cat #: C7657)
148 dissolved in HBSS buffer (Corning, Cat #: 21-020-CV) with phenol red through the
149 common bile duct. Inflated pancreases were excised, washed in phenol red-free HBSS
150 buffer (Gibco, Cat #: 14175-103) and digested at 37°C for 15 minutes. Islets were purified
151 from digested pancreas tissue by centrifugation in Biocoll density gradient (EMD Millipore,
152 Cat #: L6155) at 4°C, 2500rpm for 20 minutes. Purified islets were hand-picked under a

153 microscope (Leica Microsystems) and transferred into clean microcentrifuge tubes. Islets
154 were washed 3 times in ice-cold PBS (Corning, Cat #: 21-031-CV) at 4°C, 500xg for 2
155 minutes and stored at -20°C for ICP-MS metal analysis or used for GSIS experiments as
156 described.
157
158 **Islet perifusion**
159 Islet perifusion was performed by MMPC Core Facility, Vanderbilt University, Tennessee.
160 In brief, following isolation, islets were handpicked under the microscope for functional
161 assessment. Islet function was assessed by perifusion using approximately 50 islets (~55
162 islet equivalents (IEQ)/per perifusion chamber) at a baseline of 5.6mM glucose, and
163 stimulated with 16.7mM glucose, 16.7mM glucose + 100μM 3-isobutyl-1-methyl-xanthine
164 (IBMX, Sigma, Cat #: I5879), 16.7mM glucose + 20mM Arginine/HCl (Sigma, Cat #:
165 A6969), 5.6mM glucose + 300μM Tolbutamide (Sigma, Cat #: T0891), and 5.6mM
166 glucose + 20mM KCl. Perifusate fractions were collected at the flow rate of 3ml/min and
167 insulin was measured using radioimmunoassay kit (Millipore, Cat #: RI-13K). Insulin
168 secretion were normalized to IEQ.
169
170 **Measurement of islet and blood metal content**
171 Measurements of islet Cd were performed as previously reported (Wong, Allen et al.
172 2017). In brief, 100 islets or 30μl of blood was collected in metal-free, trace metal grade,
173 HCl-washed, 1.7ml polypropylene tubes (Denville, Cat #: C-2170). Ceramic scissors and
174 plastic instruments were used for tail nicking and blood collection. Blood and islet
175 samples were dried and heated at 80°C for 30 minutes. Dried blood and islet samples

176 were dissolved in ultra trace elemental grade (TEG) 68% HNO_3 (Fisher Scientific, Cat #:
177 A467-500), heated to 80°C for 30 minutes followed by dilution with trace metal grade
178 water (EMD, Cat #: WX0003-6) and stored at -20˚C. Samples were further diluted with
179 trace metal grade water acidified with TEG HNO_3 to a final concentration of 2.765N prior
180 to submission for Inductively Coupled Plasma Mass Spectrometry (ICP-MS) analysis, as
181 previously reported (Wong, Allen et al. 2017). Islet metal concentrations were normalized
182 to total islet protein. Total islet protein in hydrolyzed samples was measured using a BCA
183 assay kit (Thermo Scientific, Cat #: 23235) following pH neutralization with NaOH.
184 Accuracy of BCA assay protein measurements using this procedure was validated using
185 BSA standards. Negative ICP-MS output values were imputed to zero. Certified metal-
186 free pipette tips (VWR, Cat #: 53508-918), conical tubes (VWR Cat #: 89049-170, 89049-
187 174) and 1.7ml polypropylene microcentrifuge tubes (Denville, Cat #: C-2170) were used
188 throughout the collection and analysis process. All steps were performed in an epoxy-
189 coated laminar flow hood with trace element grade air filter (Baker, UK).
190

191 **^{67}Zn turnover in MIN6 cells**

192 MIN6 cells, an immortalized murine β-cell line (ATCC, Menassas, VA) (Miyazaki, Araki et
193 al. 1990) were exposed to either vehicle or 0.5μM $CdCl_2$ for 48 hours as previously
194 described (El Muayed, Raja et al. 2012). Growth media was supplemented with 10μM
195 $ZnCl_2$ to achieve a total Zn^{2+} concentration of 15μM in culture (native media contains 5μM
196 Zn^{2+}). This exposure regimen results in significant accumulation of Cd (El Muayed, Raja
197 et al. 2012). Cells were harvested 48 hours after the start of Cd exposure. At 1, 2 or 4
198 hours prior to harvest, culture media was changed and fresh media containing the rare,

199 non-radioactive ^{67}Zn tracer was added as $^{67}ZnCl_2$ at a concentration of 10μM (in addition
200 to the 5μM natural Zn mix found in media = 66.6% ^{67}Zn). At harvest, samples were
201 washed twice in PBS and incubated in 0.05% trypsin containing 0.5mM EDTA (37°C, 4
202 min, Gibco Cat #: 25300054). Following trypsinization, samples were transferred into
203 fresh microcentrifuges tubes, centrifuged (500 RCF, 3 min) and further washed twice with
204 PBS. Pellets were stored at -20°C until processed for metal profile including Zn isotopes
205 by ICP-MS. The rate of divalent ^{67}Zn uptake was used as a proxy measure for Zn turnover.
206

207 **Statistical analysis**

208 Area Under the Curve (AUC) for glucose and insulin curves during GSIS were calculated
209 using the trapezoid rule. Two-tailed t-tests were performed to compare differences
210 between control and test groups (Prism, v9.3.1). One way ANOVA with post hoc Tukey's
211 test for multiple comparison was performed to compare differences between more than
212 two groups. Where appropriate, two-way ANOVA with repeated measures was
213 performed to compare glucose and insulin secretion over time (Prism, v9.3.1). Linear
214 regression analysis was performed between islet Cd levels, islet Zn levels, glucose AUC
215 and insulin AUC in both male and female datasets (SAS). Values are expressed as mean
216 ± standard error of the mean (SEM). $p<0.05$ were considered statistically significant.
217

218 **Results**

219 **Development of the newly established *in vivo* Cd exposure-washout model**

220 In an initial pilot experiment, we exposed male C57BL/6N mice to either vehicle (V) or
221 1mM $CdCl_2$ in drinking water continuously for 12 months while being fed normal chow.

222 There were no differences in either glucose tolerance, glucose area under the curve or
223 body weight between Cd-exposed and V controls in this initial model of Cd exposure
224 without diet-induced insulin resistance (Suppl. Fig 1A-C, not included in Table 1). Next,
225 we performed experiments aimed at examining the effects of Cd exposure with high fat
226 diet-induced insulin resistance (Ayala, Samuel et al. 2010). To ameliorate the well
227 described anorexigenic effects of Cd, we employed an initial Cd exposure phase, during
228 which mice were exposed to either 0.5mM or 1mM $CdCl_2$ in their drinking water to induce
229 Cd tissue accumulation to environmentally relevant levels, followed by a washout phase
230 (without Cd exposure). The purpose of the washout phase is to mitigate the anorexigenic
231 and other systemic effects of Cd at the time of phenotyping. This is a metabolic study
232 and body weight is an important parameter that affects and/or influences metabolic
233 outcomes. Initial cohorts employed high fat diet (HFD, 42% fat) throughout the exposure
234 and washout phases (Table 1, Cohorts 2-4). Later cohorts employed regular chow during
235 the exposure phase and transitioned to HFD only during the washout phase in order to
236 induce weight gain closer to the timepoint of phenotyping (Table 1, Cohorts 5-7). Animal
237 cohorts and their experimental parameters that were performed in this study are
238 summarized in Table 1. All diets employed in the current study were analyzed and found
239 to be low in Cd content (Suppl. Table 3). The high fat diet had lower Zn concentration
240 compared to the regular chow.
241

242 ***In vivo* islet and blood Cd kinetics**

243 Initial experimental cohorts were aimed at establishing the *in vivo* kinetics of Cd in blood
244 and pancreatic islets. To do this, we exposed male mice to either V or 1mM $CdCl_2$ for 4

245 weeks followed by a washout phase (without High Fat Diet (HFD)) and measured Cd
246 levels in blood and pancreatic islets over the course of both the exposure and washout
247 phases to establish islet Cd accumulation and elimination kinetics (Table 1, Cohort #1).
248 Following 4 weeks of Cd exposure, we observed a significant increase in both islet Cd
249 accumulation (79.40 ± 3.40nmol/g protein vs 0.27 ± 0.05nmol/g protein, $p<0.001$, Fig 1A)
250 and systemic blood Cd (0.9434 ± 0.0078μM vs 0.0033 ± 0.0003μM, $p<0.001$, Fig 1B) in
251 Cd-exposed mice compared to V controls. However, at 16 weeks into the washout phase
252 (without HFD), we continue to observe an increase in islet Cd accumulation (Fig 1A) but
253 with systemic blood Cd levels (Fig 1B) returning to near baseline levels in Cd-exposed
254 mice. Overall, this demonstrates that the bioaccumulated Cd in murine islets as a
255 consequence of oral Cd exposure *in vivo* remains and persists in islets long after the
256 cessation of Cd exposure despite the return of systemic Cd levels to baseline. For
257 comparison, Cd concentration median and range found in native human islets are
258 26.1nmol/g protein and 4.4-94.7nmol/g protein respectively (Wong, Allen et al. 2017).
259 Therefore, islet Cd concentrations are comparable but lower than the high end of
260 concentrations found in human islets from the general US population (Wong, Allen et al.
261 2017). Aiming to achieve islet Cd concentration towards the upper end of those found in
262 human islets, we exposed a separate cohort of male mice with either V or 1mM $CdCl_2$ in
263 their drinking water for 19.5 weeks followed by a washout phase (Table 1, Cohort #5).
264 HFD was introduced in this cohort to assess Cd kinetics and weight trajectory under diet-
265 indued hypercaloric conditions. We euthanized two subgroups of mice at 3 and 15 weeks
266 into the washout phase. At 3 weeks into the washout phase, both islet Cd ($p<0.001$, Fig
267 1C) and blood Cd levels (Fig 1D) were elevated in Cd-HFD mice compared to V-HFD

268 controls. At 15 weeks into the washout phase, islet Cd levels remain significantly elevated
269 in Cd-HFD mice ($p<0.01$, Fig 1C) while systemic Cd levels returned to near baseline
270 values ($p<0.05$, Fig 1D) when compared to V-HFD controls. Islet Cd bioaccumulation in
271 Cd-HFD mice at both 3 and 15 weeks into the washout phase were observed in the
272 absence of significant differences in islet content of Zn, an essential metal that shares
273 many of the transport and buffering pathways with Cd (Fig 1E). Body weight gain were
274 similar between V-HFD and Cd-HFD groups throughout the exposure and washout
275 phases with the exception of one time point towards the end of the Cd exposure phase
276 (Fig 1F, $p<0.05$, 33.5 ± 2.4 g vs 29.8 ± 2.6 g for V-HFD and Cd-HFD groups respectively).
277 As a consequence, we determined that the best time to introduce the washout phase is
278 just prior to the development of the Cd-induced weight loss observed in Cd-exposed mice
279 i.e. between 17-19 weeks of Cd and to restrict the HFD feeding to the washout phase
280 while using regular chow during the Cd exposure phase. As expected in the setting of
281 lower body weight at the end of the exposure period, Cd-exposed mice showed a lower
282 glucose curve during glucose-stimulated insulin secretion (GSIS) at the end of the Cd
283 exposure phase compared to V control mice (Suppl. Fig 3A-E).
284

285 **Cadmium results in transient impairment in glucose clearance in the setting of**
286 **insulin resistance**

287 To examine the effects of islet Cd accumulation in the setting of insulin resistance in our
288 exposure-washout model, we exposed male mice to either V (n=7) or 1mM $CdCl_2$ (n=6)
289 in their drinking water simultaneously with HFD. Mice were exposed to V or Cd for 19.1
290 $\pm$ 0.7 weeks followed by a washout phase (Table 1, Cohort #2). During the washout

291 phase, Cd-exposed mice were placed on vehicle drinking water and both mice groups
292 continue to receive HFD. To characterize the metabolic parameters during the washout
293 phase, we performed metabolic studies in the same cohort of mice at two washout time
294 points (about 12 and 24 weeks into the washout phase). At 11.4 ± 0.1 weeks into the
295 washout phase with HFD, we performed GSIS (3g/kg ip glucose challenge) in both the V
296 and Cd-exposed mice. Cd-HFD mice showed higher glucose values ($p<0.05$, Fig. 2A,
297 $p<0.01$ Fig. 2B) without changes in either plasma insulin (Fig. 2C) or fasting body weight
298 (Fig. 2D). However, at 24 weeks into the washout phase with HFD, Cd-HFD mice did not
299 show differences in glucose levels following a glucose tolerance test (Fig. 2E, 1g/kg ip
300 glucose challenge, insulin not measured, per standard glucose tolerance test protocol
301 (Ayala, Samuel et al. 2010). Another cohort of male mice underwent the same procedure
302 with 1mM $CdCl_2$ exposure for 19 weeks followed by GSIS after a longer washout period
303 of 28.9 ± 0 weeks and islet isolation at 31.3 ± 0.1 weeks (Table 1, Cohort #3). As with
304 our initial experiments (Fig. 1C), islet Cd (53.6 ± 9.4nmol/g protein, $p<0.001$, Fig. 2F) in
305 Cd-HFD mice remained elevated compared to V-HFD controls at 31 weeks into the
306 washout phase despite systemic Cd levels being close to baseline (-0.0316 ± 0.0004μM
307 vs. 0.06 ± 0.03μM, $p<0.01$, Fig. 2G). A significantly lower plasma insulin level (Suppl. Fig
308 4B) during GSIS was observed in Cd-HFD mice (insulin AUC 57.3 ± 6.6 ng/mL*min)
309 compared to V-HFD controls (88.9 ± 10.1ng/mL*min) (Suppl. Fig 4D, $p<0.05$) without
310 changes in either plasma glucose levels (Suppl. Fig 4A) or fasting body weight (Suppl.
311 Fig 4E). We exposed a subsequent female cohort to a lower $CdCl_2$ concentration of 0.5
312 mM in drinking water for 18 weeks followed by a washout period with HFD feeding for
313 35.9 weeks (Table 1, Cohort #4). The lower exposure dose was chosen to account for

314 the higher bioavailability of Cd in females. Here, a significantly lower plasma insulin value
315 at 15 minutes (Suppl. Fig 6B) and a trend to a lower insulin AUC (Suppl. Fig 6D) during
316 GSIS was observed. The islet Cd bioaccumulation was fond to be markedly lower than
317 in males exposed to the 1 mM $CdCl_2$ concentration. We therefore employed a higher Cd
318 exposure concentration of 1mM for future experiments in females.
319
320 **Islet cadmium bioaccumulation reduces plasma insulin during hyperglycemic**
321 **clamp without significant changes in *ex vivo* islet insulin secretion**
322 Next, we investigated the effects of islet Cd bioaccumulation on insulin and glucose
323 homeostasis in the setting of insulin resistance. To do this, we exposed age-matched,
324 male mice to either vehicle (n=6) or 0.5mM $CdCl_2$ (n=7) in drinking water and fed regular
325 chow for 17 weeks (Table 1, Cohort #5). At the end of 17 weeks Cd exposure, Cd-
326 exposed mice were transitioned to regular vehicle water (i.e. washout phase) with HFD
327 for 12 weeks prior to standard hyperglycemic clamp studies (Ayala, Samuel et al. 2010).
328 In the setting of hyperglycemia, maintained at 250-300mg/dL arterial glucose (Fig. 3A) by
329 continuous glucose infusion (Fig. 3B), Cd-exposed mice on HFD (Cd-HFD) showed lower
330 plasma insulin levels compared to V mice on HFD (V-HFD) at 120 min ($p<0.05$, Fig. 3C).
331 The decrease in plasma insulin observed in Cd-HFD mice during hyperglycemic clamp
332 occurred in the absence of changes in either plasma c-peptide (Fig. 3D) or body weight
333 (Fig. 3E). To assess Cd accumulation on *ex vivo* islet insulin secretion, we performed
334 islet perifusion and stimulation with glucose and several insulin secretagogues in islets
335 from V-HFD (n=5) and Cd-HFD (n=5) mice. Islet insulin release (Fig. 3F) and total islet
336 insulin content (Fig. 3G) were similar between Cd-HFD and V-HFD control islets in

337 response to 16.7mM glucose, 100uM BMX, 20mM Arginine, 300uM Tolbutamine and
338 20mM KCl. This suggests that the mechanisms of Cd-induced decrease in plasma insulin
339 observed during hyperglycemic clamp is independent of changes in the rate of insulin
340 secreted per islet or that the *in vivo* milieu is relevant for the Cd's effect.
341

342 **Gender dichotomy of cadmium-mediated glycemic effects *in vivo***

343 Next, we investigated the gender dichotomy of Cd-mediated glycemic effects. To do this,
344 we exposed age-matched, male (Table 1, Cohort 7a) and female (Table 1, Cohort 7b)
345 mice in parallel to either V (n=9-11) or 1mM $CdCl_2$ (n=9-10) dose in drinking water for
346 17.8 ± 0.1 weeks. Cadmium-exposed mice were transitioned to vehicle drinking water
347 following 17.8 ± 0.1 weeks of Cd exposure during the washout phase. Both groups of V
348 and Cd-exposed mice received regular chow during the Cd exposure phase and HFD
349 (42% from fat) during the washout phase. Following the Cd exposure phase and prior to
350 the washout phase, V and Cd-exposed, male mice did not display any differences in
351 whole body glucose clearance (Fig. 4A) and GSIS (Fig. 4B). In contrast, Cd-exposed
352 female mice displayed significantly higher plasma insulin levels 30 minutes after a
353 glucose load compared to their V controls ($p<0.05$, Fig. 4B). This increase in plasma
354 insulin was not associated with changes in either whole-body glucose clearance (Fig. 4A)
355 or fasting body weight (Fig. 4C). Following 19.1 ± 0.1 weeks into the washout phase with
356 HFD, we did not observe significant differences in glucose values or plasma insulin during
357 GSIS between V-HFD and Cd-HFD males (Figs. 4D-F), a different result compared to
358 prior Cohorts #2 and #3 which received HFD during the Cd exposure phase. In contrast,
359 following the same washout period (19.0 ± 0.8 weeks), we observe a significantly higher

360 whole-body glucose clearance (i.e. lower glucose levels) in Cd-HFD females compared
361 to their V-HFD control counterparts ($p<0.05$, Fig. 4D and 4E). This increase in whole
362 body glucose clearance in Cd-HFD females was not associated with changes in either
363 plasma insulin (Fig. 4F) or fasting body weight (Fig. 4G). There were also no significant
364 differences in GSIS between Cd-HFD and V-HFD females at 34 weeks into the washout
365 phase (Suppl. Fig 5A-E). Islets from Cd-HFD female mice showed significant islet Cd
366 bioaccumulation (119.3 $\pm$ 14.0nmol/g protein) compared to their V-HFD female controls
367 (29.3 $\pm$ 17.3nmol/g protein) ($p<0.01$, Fig. 4H). While islet Cd in V-HFD female controls
368 was significantly lower, it was still markedly higher (29.3 $\pm$ 17.3nmol/g protein, $p<0.01$,
369 Fig. 4H) than V-HFD in males from Cohorts #1, 2, 3 and 5 (Table 1). It is of note that
370 serum creatinine levels in Cd-HFD animals were not significantly different to that of the
371 V-HFD group (Suppl. Table 1) suggesting that this regiment of Cd exposure (1mM $CdCl_2$
372 for 18 weeks followed by washout and HFD for 26 weeks) did not affect kidney function,
373 which is an important consideration when interpreting dysglycemia data given that renal
374 failure results in prolonged half-life of insulin. There were no differences in plasma
375 proinsulin or proinsulin:insulin ratio in selected experiments (data not shown).
376

377 **Linear regression analysis and correlation between islet Cd and plasma insulin**

378 To further evaluate the relationship between Islet Cd bioaccumulation and Cd-mediated
379 dysglycemia in each gender, we performed linear regression analysis between islet Cd
380 content and insulin AUC during *in vivo* GSIS in both males and females. The aim of this
381 analysis is to explore the influence of variations in islet Cd accumulation on plasma insulin
382 given the variation in insulin values seen across cohorts. In cohorts where repeated GSIS

383 was performed, GSIS data closest to the time of islet isolation was chosen. When male
384 and female datasets were pooled and analyzed, we observed a significant gender effect
385 on insulin AUC ($p<0.05$, Table 2). We therefore repeated the linear regression analysis
386 in males and females separately. We observed that islet Cd content (independent
387 variable) was negatively associated with insulin AUC (dependent variable) during *in vivo*
388 GSIS in males ($p<0.05$, Table 2) but not in females. There was no correlation between
389 islet Zn and insulin AUC in either males or females (Table 2). The correlation between
390 insulin AUC and islet Cd as well as the gender dichotomy did not change when AUC
391 glucose was included in the model (Suppl. Table 2A). This correlation also did not change
392 in simpler models that included fewer independent variables or islet Cd alone in females
393 (Suppl. Table 2D) but not in males (Suppl. Table 2C). In males, a significant correlation
394 was observed in a model that did not include age between insulin AUC and islet Cd
395 content (Suppl. Table 2C).
396

397 ***Ex vivo* cadmium accumulation in intact murine and human islets did not result in**
398 **measurable changes in insulin secretion**

399 To compare the rate of Cd accumulation and functional impact between human and
400 murine islets, we exposed human islets (n=3/group) and mouse islets (n=6/group) to
401 either V or 0.1μM $CdCl_2$ for 48 hours in culture and measured islet Cd content. Islets
402 originating from the same donor or mouse were divided equally between parallel
403 exposure conditions. Cadmium-exposed human islets accumulated significantly higher
404 intracellular Cd levels (121.7 ± 25.8nmol/g protein) compared to vehicle control islets
405 (21.1 ± 7.0nmol/g protein) following 48 hours of Cd exposure ($p<0.05$, Fig. 5A).

406 Cadmium-exposed murine islets also showed significantly higher Cd levels (38.3 ±
407 3.0nmol/g protein) compared to vehicle control islets (7.6 ± 1.2nmol/g protein) following
408 48 hours of Cd exposure ($p<0.001$, Fig. 5A). Cadmium levels in human islets exposed to
409 Cd *ex vivo* was significantly higher compared to mouse islets exposed under the same
410 conditions ($p<0.0001$, Fig 5A). There were also no significant differences in total islet
411 proinsulin to insulin ratio in response to Cd exposure in mouse islets *ex vivo* (data not
412 shown).
413
414 ***Ex vivo* cadmium accumulation did not affect islet Zn content or β-cell Zn turnover**
415 Given that Cd has been shown to interact with many Zn transport and binding proteins
416 (Himeno, Yanagiya et al. 2009, Friedman 2014), we compared islet Zn levels following *ex*
417 *vivo* (refer to paragraph above) or *in vivo* Cd accumulation in islets. Human islets
418 contained lower Zn levels compared to mouse islets at baseline ($p<0.01$, Fig 5B),
419 suggesting significant differences in divalent metal handling between human and mouse
420 islets. However, Cd exposure did not significantly affect islet Zn content in either human
421 or mouse islets (Fig 5B). Next, we examined the turnover of Zn following Cd accumulation
422 in immortalized murine β-cell line MIN6. Cell culture, Cd exposure and cell harvest were
423 performed as previously described (El Muayed, Raja et al. 2012). For this, we exposed
424 MIN 6 cells to either V or 0.5μM $CdCl_2$ in media for 48 hours. Following 48 hours of $CdCl_2$
425 incubation, media was changed and 10μM ^{67}Zn tracer was added to fresh culture media
426 (equivalent to 66% of total Zn in media) and the rate of cellular ^{67}Zn uptake was measured
427 at 1, 2 and 4 hours following the start of ^{67}Zn tracer exposure. The rate of cellular ^{67}Zn
428 uptake was used as a proxy measurement for cellular Zn turnover. We observed that the

429 rate of ^{67}Zn accumulation were similar between V and Cd-exposed MIN6 cells, suggesting
430 that cellular Cd accumulation *in vitro* did not affect cellular Zn turnover (Suppl. Fig. 2).
431 Overall, islet Zn content was not significantly different between Cd-HFD mice and V-HFD
432 controls from any of our animal cohorts (Table 1).
433

434 **Discussion**

435 Here, we report the development of a chronic, oral Cd exposure mouse model that results
436 in islet Cd bioaccumulation that is comparable to that found in human islets from the
437 general US population (Wong, Allen et al. 2017). In males, exposure to 1mM $CdCl_2$ in
438 drinking water for 19 weeks followed by washout with HFD resulted in islet Cd
439 bioaccumulation that is associated with decrease glucose tolerance at 11 weeks and
440 decrease plasma insulin at 28 weeks into the washout phase in the absence of changes
441 in *ex vivo* islet insulin secretion, body weight or renal function. In contrast, Cd exposure
442 in female mice to the same conditions was associated with islet Cd bioaccumulation and
443 elevated plasma insulin during GSIS without changes in whole body glucose clearance
444 immediately following Cd exposure (prior to washout phase). However, following the
445 washout phase with HFD, Cd-HFD females displayed lower systemic glucose clearance
446 during GSIS without changes in either plasma insulin or body weight despite achieving
447 comparable islet Cd concentrations. A relatively wide variation in islet Cd accumulation
448 was observed between individual mouse. This also included a relatively high level of Cd
449 in female vehicle-exposed islets in cohort 7b. It is likely that variation in consumption of
450 $CdCl_2$-containing water as well as varied oral bioavailability and tissue distribution are

451 factors contributing to this. Additionally, variations in the content of Cd and other metals
452 in rodent chows may have contributed to the observed variations.
453
454 Results from the regression analysis showed the close relationship between islet Cd
455 plasma insulin levels during *in vivo* glucose-stimulated insulin secretion experiments,
456 providing additional evidence for the functional impact of Cd accumulation at
457 environmentally relevant concentrations on *in vivo* beta-cell function. At the same time,
458 this relationship indicates that variations in the observed effect of Cd exposure across
459 cohorts and within cohorts are at least partially explained by variations in islet Cd
460 accumulation. There are several benefits to our oral exposure-washout *in vivo* mouse
461 model. Firstly, it ameliorated the anorexigenic effects of Cd, thereby resulting in a similar
462 mean body weight gain between V and Cd-exposed animals throughout the study. The
463 *in vivo* anorexigenic effects of Cd was mitigated with the washout phase following Cd
464 exposure in our model. Secondly, this oral exposure-washout regiment achieves target
465 tissue (pancreatic islets) Cd bioaccumulation at concentrations comparable to those
466 found in human islets while reducing systemic blood Cd concentrations at the end of the
467 washout phase and minimizing generalized systemic toxic effects. Islet Cd range in Cd-
468 exposed mice is consistent with islet Cd range that we have previously reported in human
469 islets (4.4 - 94.7nmol/g protein) (Wong, Allen et al. 2017), hence making this *in vivo*
470 experimental Cd dose relevant in the context of human environmental Cd exposure.
471 Furthermore, the continued oral Cd exposure through drinking water was employed to
472 resemble environmental exposure routes seen in the general population. The oral Cd
473 dose of 1mM was chosen to compensate for low oral Cd bioavailability and life-long tissue

474 accumulation as reported in humans (Jarup, Rogenfelt et al. 1983, Schilderman, Moonen
475 et al. 1997).
476
477 Several epidemiological studies have described contradictory findings between Cd
478 exposure and dysglycemia. Some have reported a statistically significant, positive
479 association between Cd exposure and dysglycemia (Schwartz, Il'yasova et al. 2003,
480 Wallia, Allen et al. 2014, Nie, Wang et al. 2016) while others have reported the lack of a
481 statistically significant association (Barregard, Bergstrom et al. 2013, Moon 2013, Menke,
482 Guallar et al. 2016). Discrepancies in observations could be attributed to differences in
483 study design, study power, sample analyzed (blood or urine), genetics and population
484 exposure levels. Inconsistencies between Cd exposure and dysglycemia have also been
485 reported in Cd-induced diabetic animal models. Some studies have shown that *in vivo*
486 Cd exposure resulted in hyperglycemia and β-cell dysfunction (Chang, Hsu et al. 2013,
487 Trevino, Waalkes et al. 2015, Huang, Kuo et al. 2019, Fitzgerald, Olsen et al. 2020, Hong,
488 Xu et al. 2021) while others have demonstrated normal glucose homeostasis with modest
489 decrease in insulin secretion following Cd exposure *in vivo* (Li, Li et al. 2019). Trevino *et*
490 *al* (2015) and Fitzgerald *et al* (2020) used a lower Cd dose of 32.5ppm and 0.6ppm in
491 their exposure rat models respectively. Animal strain, dose, duration and route of
492 administration of Cd should be considered when interpreting data reported in Cd-induced
493 animal models of dysglycemia. Additionally, short duration Cd exposure may result in
494 acute systemic toxic effects especially with elevated blood Cd levels in the absence of a
495 washout period. Given the diverse intracellular targets of Cd, each with a different
496 concentration-effect relationship, it is not surprising that Cd effects that are observed at a

497 whole cell and organism level are strongly dependent on exposure duration and tissue
498 concentration.
499
500 Pancreatic β-cells accumulate Cd in a dose- and time-dependent manner *in vitro* (El-
501 Muayed, Raja et al. 2012). Measurable levels of Cd have also been detected in human
502 islets (Wong, Allen et al. 2017). However, the molecular mechanisms of Cd^{2+} transport
503 into β-cells are largely unknown. DMT1 (Lortz, Schroter et al. 2014), ZnT (Kambe, Narita
504 et al. 2002, Chimienti, Favier et al. 2005, Cai, Kirschke et al. 2018) and ZIP (Lawson,
505 Maret et al. 2017) are metal transport proteins that are abundantly expressed in
506 pancreatic β-cells. A known iron transporter, DMT1 has been reported to also effectively
507 transport several other divalent metals such as Fe^{2+}, Mn^{2+}, Ni^{2+}, $Co^{2+}$and Cd^{2+} (Tallkvist,
508 Bowlus et al. 2001, Arredondo, Munoz et al. 2003, Garrick, Dolan et al. 2003). ZIP and
509 ZnT are known to facilitate Zn^{2+} entry into and exit from the cytosol respectively (Lemaire,
510 Chimienti et al. 2012, Lawson, Maret et al. 2017). In addition to transporting the divalent
511 cation Zn^{2+}, some ZIP class transporters can transport Cu^{2+}, Ni^{2+} (Antala and Dempski
512 2012) and Mn^{2+} (Winslow, Limesand et al. 2020). The capacity to transport Cd effectively
513 has been shown for ZIP8, ZIP14 and ZnT1 (Dalton, He et al. 2005, Ohana, Sekler et al.
514 2006, Girijashanker, He et al. 2008). DMT-1, ZIP14 and ZIP8 are highly expressed in
515 murine and human islets (Mohanasundaram, Drogemuller et al. 2011, Hansen, Tonnesen
516 et al. 2012, Coffey and Knutson 2017, Lawlor, George et al. 2017, Wong, Wang et al.
517 2021).
518

519 We have previously shown that the accumulation of Cd in β-cells at environmentally
520 relevant levels leads to impaired β-cell function *ex vivo* (El-Muayed, Raja et al. 2012).
521 These experiments were carried out in dispersed murine islets as well as in an
522 immortalized murine β-cell line, MIN6. In contrast, our current experiments did not show
523 any differences in *ex vivo* function of intact islets following either *in vivo* or *ex vivo* Cd
524 accumulation. It is likely that this difference is due to a protective effect of an intact islet
525 structure. We also observed a higher rate of *ex vivo* Cd accumulation in human islets
526 compared to mouse islets, possibly due to differences in the composition and function of
527 metal transporters (especially divalent metal transporters) between human and mouse
528 islets. This observation highlights the value of assessing tissue level Cd concentrations
529 when evaluating its toxic effects. Accumulation of Cd *in vivo* have been associated with
530 hyperglycemia and decrease glucose-stimulated insulin secretion in a model of shorter
531 term exposure (Fitzgerald, Olsen et al. 2020). The addition of a washout phase in our
532 current model provides the added advantage of mitigating acute toxic effects of Cd,
533 thereby facilitating a better correlation between target tissue Cd levels and its resulting
534 toxic effects.
535
536 The underlying molecular mechanisms of intracellular Cd bioaccumulation on β-cell
537 cytotoxicity and function are not well studied. Chang et al. (2013) showed that intracellular
538 Cd accumulation *in vitro* resulted in β-cell apoptosis that is mediated by the JNK-regulated,
539 mitochondria-dependent pathway (Chang, Hsu et al. 2013). Cadmium-mediated
540 pancreatic β-cell death was also shown to be mediated by Ca^{2+}-dependent, JNK
541 activation and CHOP-related signaling pathways (Huang, Kuo et al. 2019). It has also

542 been hypothesized that Cd may interfere with the trafficking of Zn in β-cells given the high
543 Zn turnover present in β-cells and the overlap between Cd and Zn transport pathways.
544 However, the lack of change in islet Zn concentration in response to Cd accumulation
545 provides evidence against this hypothesis, at least at the whole cell level. However, this
546 does not rule out changes in Zn distribution within cells at the protein or organelle level in
547 response to Cd accumulation. Taken together, our current findings and published
548 literature indicate that accumulation of Cd in pancreatic islets at environmentally relevant
549 concentrations that are in the range found in human islets (Wong, Allen et al. 2017) is
550 cytotoxic to β-cells, thus resulting in Cd-mediated β-cell changes that consequently
551 affects total insulin secretory capacity *in vivo*. Therefore, the current study adds to prior
552 epidemiologic and experimental evidence that members of the general population are
553 exposed to environmental Cd levels that are likely to contribute to β-cell failure, thereby
554 increasing the risk for type 2 diabetes. Consequently, the diabetogenic effect of Cd
555 should be taken into account when setting Cd exposure limits.
556
557 Cadmium-mediated molecular mechanisms *in vivo* and *ex vivo* are likely distinct from one
558 another which, in turn, could affect Cd toxicology differently under both conditions. This
559 may be due to the uptake, organification and toxicokinetic properties of Cd. *In vivo*, Cd
560 is primarily bound to albumin or metallothionein (Jin, Nordberg et al. 1986, Nordberg
561 2004). *Ex vivo*, the primary form of Cd in culture is Cd^{2+}. Recently, we reported
562 differences in Cd-mediated islet transcriptome changes between *in vivo*- and *ex vivo*-
563 exposed islets where we did not find any overlap in Cd-induced differentially expressed
564 genes in both groups (Wong, Wang et al. 2021). While our model shows several

565 advantages over other approaches, several drawbacks have to be acknowledged. Firstly,
566 these experiments are time-consuming and resource-intensive. Secondly, the observed
567 variation in islet Cd accumulation and resulting variations in observed changes in plasma
568 insulin presents a drawback. Despite this, we believe this model to be a good tool for
569 studying the degree and mechanisms underlying the diabetogenic effect of Cd and other
570 persistent toxicants that accumulate in insulin-producing islets.
571
572 Here, we report the development of a chronic, oral Cd exposure mouse model that results
573 in islet Cd bioaccumulation that is relevant in the context of environmental Cd exposure
574 in humans. Our *in vivo* Cd exposure-washout mouse model showed islet Cd
575 bioaccumulation that is associated with subtle and complex Cd-mediated effects on
576 glucose clearance and plasma insulin levels. Further research examining the relationship
577 between Cd exposure, islet Cd bioaccumulation, dysglycemia and their underlying
578 mechanisms are needed to understand the effects of Cd-mediated β-cell dysfunction.
579

580 **Acknowledgements**

581 ICP-MS metal analysis was performed at Quantitative Bio-elemental Imaging Center,
582 Northwestern University that is supported by NASA Ames Research Center
583 (NNA04CC36G). The authors thank the Vanderbilt MMPC Core Facility (U24 DK059637)
584 for performing hyperglycemic clamps and islet perifusion studies.

585

586 **Funding**

587 This research was supported by grants from the National Institutes of Health/National
588 Institute of Environmental Health Sciences (5R01ES027011 and 5K08ES020880)
589 awarded to MEM and the National Institutes of Health/National Center for Advancing
590 Translational Sciences (UL1TR001422).

591

592 **Declaration of competing interest**

593 The authors declare that they have no known competing financial interests or personal
594 relationships that could have appeared to influence the work reported in this paper.

595

596 **Authors' contributions**

597 Winifred Wong: Conceptualization, Investigation, Validation, Formal analysis, Writing –
598 original draft, review and editing. Janice Wang: Investigation, Validation, Writing-review
599 and editing. Matthew Meyers: Investigation. Nathan Wang: Investigation. Rebecca
600 Sponenburg: Investigation. Norrina Allen: Formal analysis. Joshua Edwards: Writing
601 – review and editing. Malek El-Muayed: Conceptualization, Investigation, Formal

602 analysis, Funding acquisition, Writing-review and editing. All authors have read and
603 approved the final manuscript.
604

605 **List of Figures**

606 Fig. 1: (A) Islet Cd content (normalized to total islet protein) and (B) blood Cd levels in
607 male mice exposed to either V (n=4-5) or 1mM $CdCl_2$ (n=4-8) for 4 weeks followed by 16
608 weeks of washout (Table 1, Cohort #1). (C) Islet Cd content, (D) blood Cd levels, (E) islet
609 Zn content and (F) body weight curve in male mice exposed to either V (n=3-6) or 1mM
610 $CdCl_2$ (n=3-6) for 19.5 weeks on regular chow followed by 3 and 15 weeks washout with
611 high fat diet (HFD, Table 1, Cohort #5). V-HFD, Vehicle-exposed followed by washout
612 and HFD; Cd-HFD, Cd-exposed followed by washout and HFD. Data are expressed as
613 mean ± SEM. *$p<0.05$, **$p<0.01$, ***$p<0.001$.

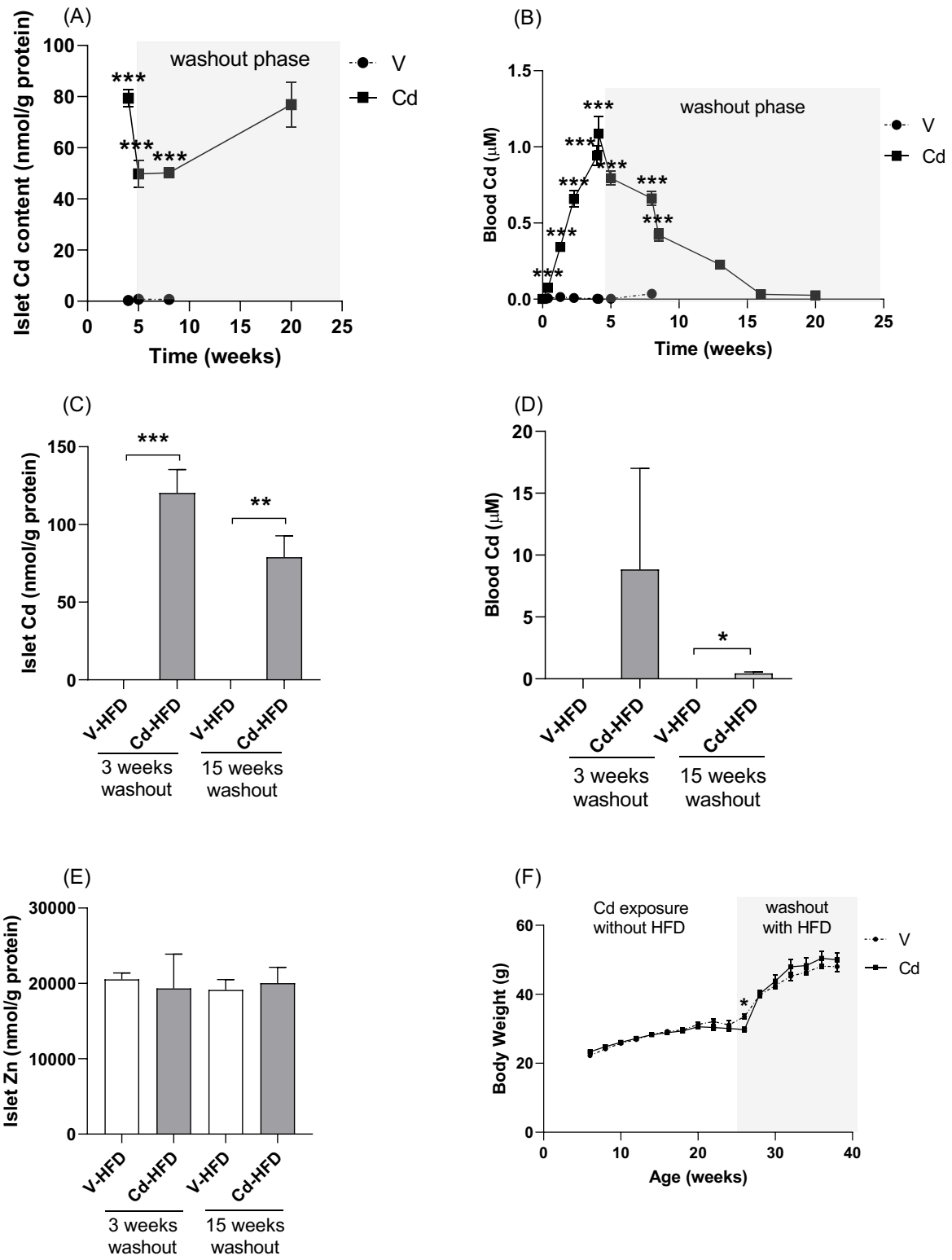
(A)
washout phase
V
Cd
Islet Cd content (nmol/g protein)
Time (weeks)
(B)
washout phase
V
Cd
Blood Cd (μM)
Time (weeks)
(C)
Islet Cd (nmol/g protein)
V-HFD
Cd-HFD
V-HFD
Cd-HFD
3 weeks washout
15 weeks washout
(D)
Blood Cd (μM)
V-HFD
Cd-HFD
V-HFD
Cd-HFD
3 weeks washout
15 weeks washout
(E)
Islet Zn (nmol/g protein)
V-HFD
Cd-HFD
V-HFD
Cd-HFD
3 weeks washout
15 weeks washout
(F)
Cd exposure without HFD
washout with HFD
V
Cd
Body Weight (g)
Age (weeks)

614

615

616 Fig 2: (A) Blood glucose, (B) area under the curve, (C) plasma insulin and (D) fasting
617 body weight during GSIS about 11.4 ± 0.1 weeks into washout phase with HFD in male
618 mice exposed to either V (n=7) or 1mM $CdCl_2$ (n=6) for 19.1 ± 0.7 weeks with HFD. (E)
619 Blood glucose during glucose tolerance test 24 weeks into washout phase with HFD in V
620 (n=7) or Cd-exposed (n=6) male mice on HFD (Table 1, Cohort #2). (F) Islet Cd content
621 and (G) blood Cd in male mice exposed to either V (n=6) or 1mM $CdCl_2$ (n=6) for 19
622 weeks with HFD followed by 31.3 ± 0.1 weeks of washout with HFD (Table 1, Cohort #3).
623 V-HFD, Vehicle-exposed followed by washout and HFD; Cd-HFD, Cd-exposed followed
624 by washout and HFD. Data are expressed as mean ± SEM. *$p<0.05$, **$p<0.01$,
625 ***$p<0.001$.

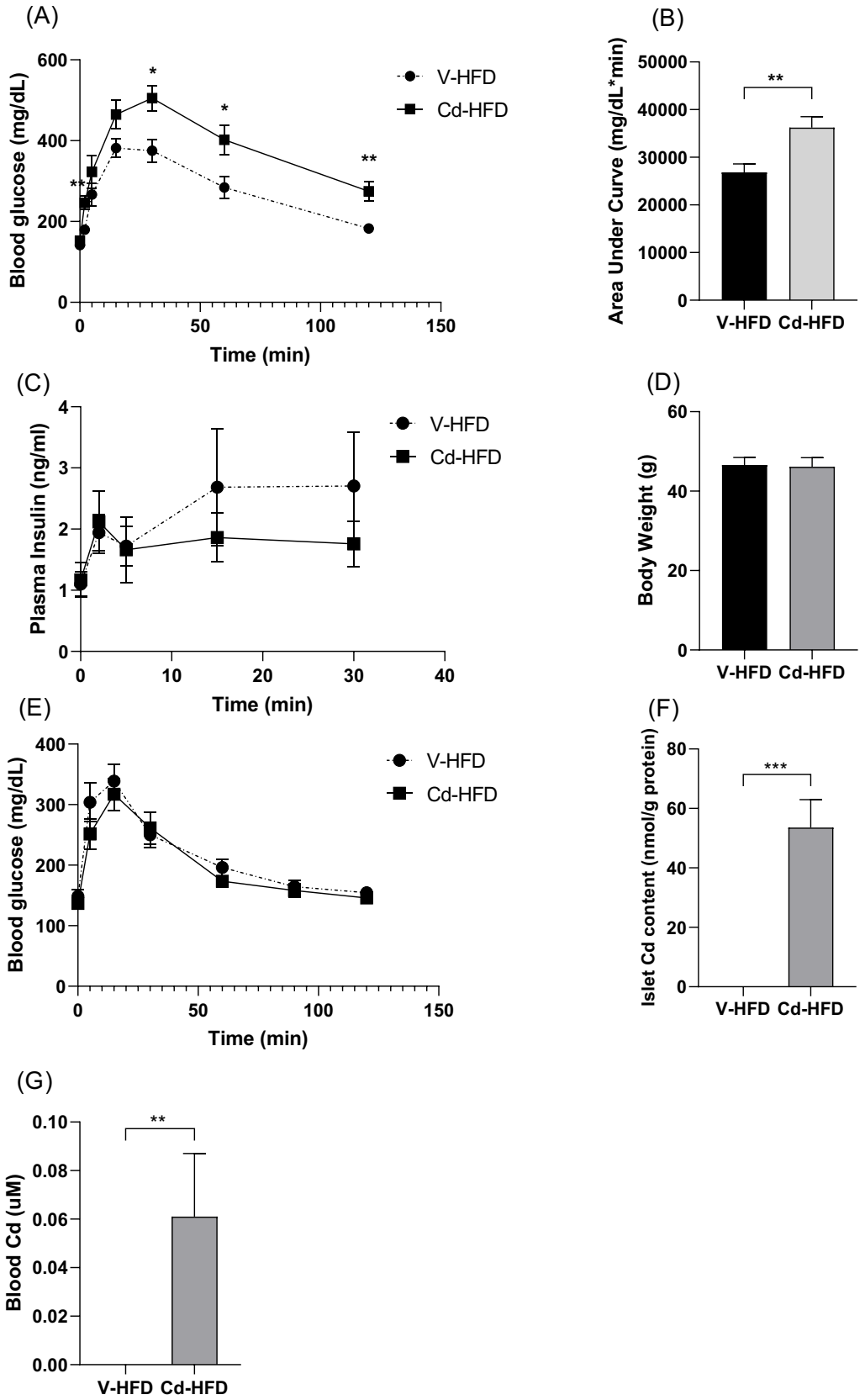
(A)
Blood glucose (mg/dL)
Time (min)
V-HFD
Cd-HFD
(B)
Area Under Curve (mg/dL*min)
V-HFD Cd-HFD
(C)
Plasma Insulin (ng/ml)
Time (min)
V-HFD
Cd-HFD
(D)
Body Weight (g)
V-HFD Cd-HFD
(E)
Blood glucose (mg/dL)
Time (min)
V-HFD
Cd-HFD
(F)
Islet Cd content (nmol/g protein)
V-HFD Cd-HFD
(G)
Blood Cd (uM)
V-HFD Cd-HFD

626

627 Fig. 3: (A) Arterial blood glucose, (B) glucose infusion rate, (C) plasma insulin, (D) plasma
628 c-peptide and (E) body weight during hyperglycemic clamp in mice exposed to either V
629 (n=6) or 0.5mM $CdCl_2$ (n=7) for 17 weeks followed by 12 weeks of washout with HFD on
630 V water (Table 1, Cohort #6). (F) Islet insulin secretion in response to high glucose and
631 several insulin secretagogues from V and Cd-exposed mice following 12 weeks of
632 washout with HFD (n=5/group). (G) Total islet insulin content following islet perifusion in
633 V and Cd-exposed mice islets following 12 weeks of washout with HFD (n=5/group). V-
634 HFD, Vehicle-exposed followed by washout and HFD; Cd-HFD, Cd-exposed followed by
635 washout and HFD. Data are expressed as mean ± SEM. *$p<0.05$.

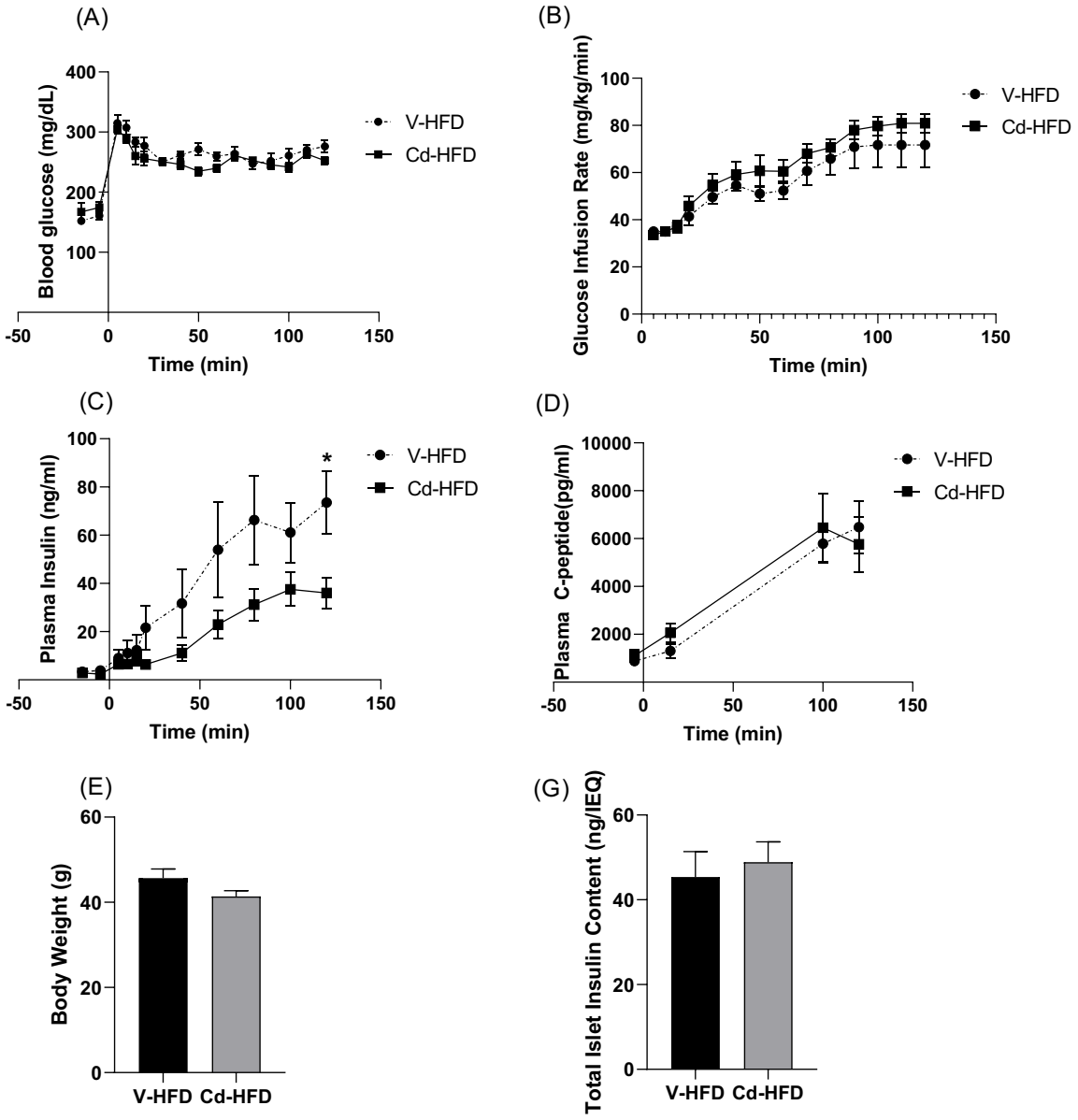

636

637

638

639

640

641

642

643

644 (F)

645

646

647

648

649

650

651

652

653

654

655

656

657

658

659

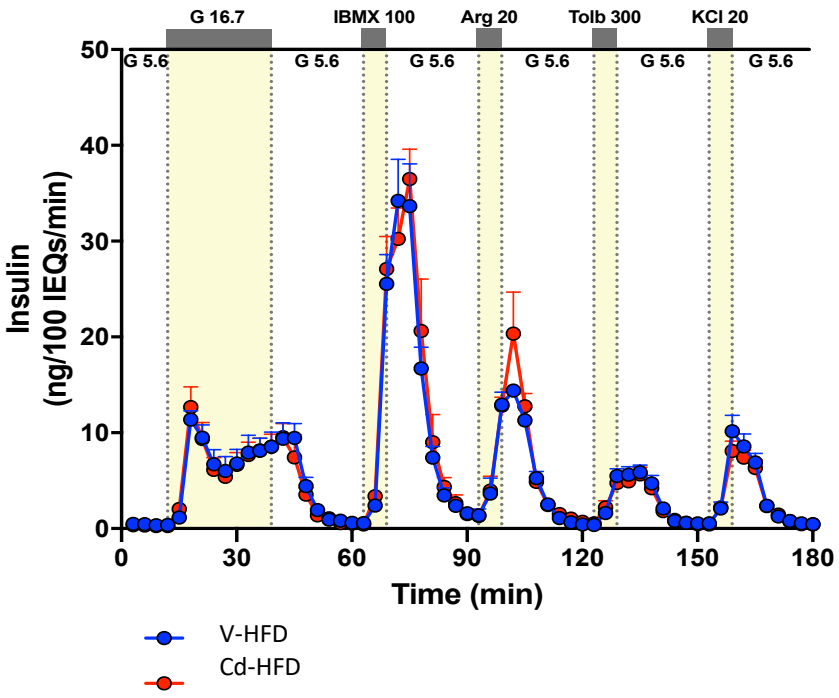

660 Fig. 4: (A) Blood glucose, (B) plasma insulin and (C) fasting body weight during *in vivo*
661 GSIS in age-matched male and female mice exposed to either V (n=10 (males), n=11
662 (females)) or 1mM $CdCl_2$ (n=10/gender) for 17.8 ± 0.1 weeks (Table 1, Cohort #7a-b). (D)
663 Glucose curve and corresponding (E) area under the curve, (F) plasma insulin and (G)
664 fasting body weight during GSIS in age-matched V-HFD and Cd-HFD male (n=9-10/group)
665 and female (n=9-10/group) mice 19.1 ± 0.1 weeks into the washout phase with HFD. (H)
666 Islet Cd content (normalized for total islet protein) at sacrifice in V-HFD (n=9) and Cd-
667 HFD (n=8) female mice. V-F, Vehicle females; Cd-F, Cd-exposed females; V-M, Vehicle
668 males; Cd-M, Cd-exposed males; V-HFD, Vehicle-exposed followed by washout and HFD;
669 Cd-HFD, Cd-exposed followed by washout and HFD. Data are expressed as mean ±
670 SEM. *$p<0.05$, **$p<0.01$.

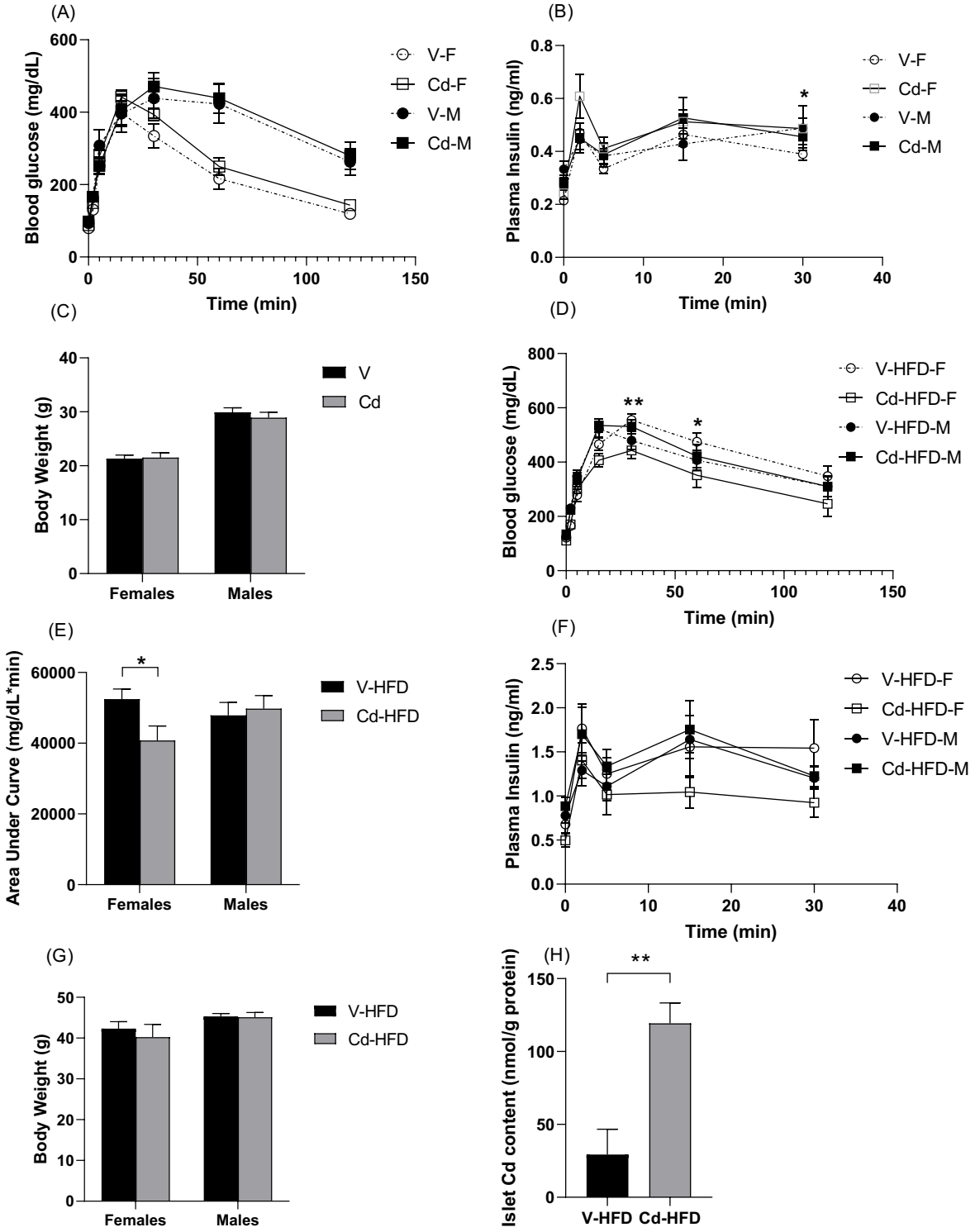
(A)
Blood glucose (mg/dL)
Time (min)
V-F
Cd-F
V-M
Cd-M
(B)
Plasma Insulin (ng/ml)
Time (min)
V-F
Cd-F
V-M
Cd-M
(C)
Body Weight (g)
Females
Males
V
Cd
(D)
Blood glucose (mg/dL)
Time (min)
V-HFD-F
Cd-HFD-F
V-HFD-M
Cd-HFD-M
(E)
Area Under Curve (mg/dL*min)
Females
Males
V-HFD
Cd-HFD
(F)
Plasma Insulin (ng/ml)
Time (min)
V-HFD-F
Cd-HFD-F
V-HFD-M
Cd-HFD-M
(G)
Body Weight (g)
Females
Males
V-HFD
Cd-HFD
(H)
Islet Cd content (nmol/g protein)
V-HFD
Cd-HFD

671

672

673 Fig. 5: (A) Islet Cd and (B) islet Zn (normalized to total islet protein) in murine (n=6/group)
674 and human islets (n=3/group) exposed to either V or 0.1μM $CdCl_2$ for 48 hours. Data are
675 expressed as mean ± SEM. Adjusted p-values from one way ANOVA with post hoc
676 Tukey's test for multiple comparison. * p<0.05, **p<0.01, ****p<0.0001, ns: not significant.

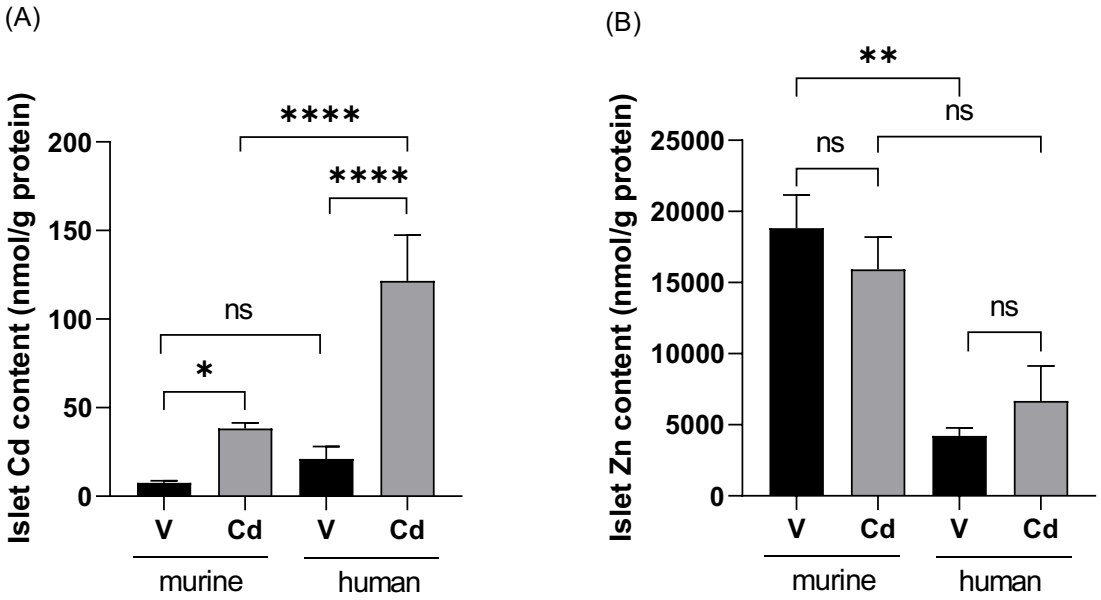

677

678

679 **List of tables**

680 Table 1: List of cohorts with their relevant experimental and islet outcome parameters. Data are expressed as mean ± SEM.

681 *p<0.05.

Cohort#	Cohort Description	Gender	Number of animals used (Cd / Vehicle)	Deaths (Cd / V)	Exposure Group $CdCl_2$ Concentration in Drinking Water	Diet During Exposure/ Diet during Washout	Vehicle Group AUC Insulin During GSIS Avg	Cd Group AUC Insulin During GSIS	Vehicle Group AUC Glucose During GSIS	Cd Group AUC Glucose During GSIS	islet Cd in V group	Islet Cd in Cd group	islet Zn in V group	Islet Zn in Cd group	Fasting Body Weight During GSIS Cd / V Group (g)	Exposure Time Prior to Washout Cd/V (weeks)	Washout Duration prior to GSIS (Cd/V, weeks)	Washout Duration prior to islet isolation (Cd/V, weeks)
1 (Fig. 1A-B)	Islet Cd Kinetics (4 Week Uptake, 1,4,16 Week Elimination)	m	21/13	0/0	1 mM	Regular/ Regular	N/A	N/A	N/A	N/A	0.27 ± 0.04, 0.78± 0.1, 0.67 ± 0.12 after 0, 1, 4 weeks washout	79.40 ± 2.9, 49.82 ± 4.6, 50.25 ± 1.8, 76.91 ± 7.5 after 0, 1, 4, 16 weeks washout	40010 ± 2451, 34710 ± 1115, 36366 ± 3227 after 0, 1, 4 weeks washout	42362 ± 1449, 25307 ± 642 , 34913 ± 775, 68449 ± 7134 after 0, 1, 4, 16 weeks washout	28.7 ± 0.6 / 29.4 ± 0.5	4 ± 0 / 4 ± 0	N/A	0,1,4, and 16
2 (Fig.. 2A-E)	Effect of Cd accumulation on markers of beta islet function in males	m	6/7	0/0	1 mM	42% fat/ 42% fat	70.98 ± 18.62	53.70 ± 10.60	**33803 ± 2119 ***	**46365 ± 2794 ***	2.50 ± 1.90	114.25 ± 31.23	49403 ± 2278	50552 ± 1788	46.1 ± 2.1 / 46.6 ± 1.8	19.6 ± 1.1 / 18.6 ± 0.8	11.5 ± 0.1 / 11.3 ± 0.1	27.3 ± 0.0/ 26.9 ± 0
3 (Fig. 2F-G, Suppl. Fig. 4)	Effect of Cd accumulation on markers of beta islet function in males (prolonged washout)	m	6/6	0/0	1 mM	42% fat/ 42% fat	**88.93 ± 10.13 ***	**57.32 ± 6.58***	44417 ± 2514	35375 ± 6152	BDL	53.58 ± 8.55	25270 ± 1434	24874 ± 2645	50.3 ± 1.2 / 53.8 ± 1.4	19 ± 0 / 19 ± 0	28.9 ± 0 / 28.9 ± 0	31.4 ± 0.1 / 31.3 ± 0.1
4 (Suppl. Fig. 6)	Effect of lower Cd exposure dose with continuous HFD in females	f	8/7	0/0	0.5 mM	42% fat/ 42% fat	63.95 ± 4.25	49.60 ± 5.23 (p=0.073)	41713 ± 4768	51546 ± 4033	BDL	30.38 ± 3.09	27330 ± 1970	30641 ± 2609	47.8 ± 1.1 / 43.7 ± 3.8	18 ± 0 / 18 ± 0	35.9 ± 0 / 35.9 ± 0	40.9 ± 0.2 / 40.9 ± 0
5 (Fig. 1C-F, Suppl. Fig3)	Islet Cd Kinetics 19.6 week uptake, 3 and 15 week washout	m	10/9	1/0	1 mM	Regular/ 42% fat	22.58 ± 2.67	17.70 ± 1.42	**55430 ± 2581***	**38835 ± 4598 ***	BDL	120.3 ± 12.2, 78.9 ± 12 after 3 and 19.6 weeks washout	20540 ± 695, 19128 ± 1133 after 3 and 19.6 weeks washout	19342 ± 3707, 20047 ± 1817 after 3 and 19.6 weeks washout	27.1 ± 0.7 / 28.7 ± 0.7	19.6 ± 0/ 19.6 ± 0	0 (no washout)	3 and 15
6 (Fig. 3A-G)	Effect of Cd accumulation on markers of beta islet function in males, lower exposure dose	m	7/6	0/0	0.5 mM	Regular/ 42% fat	N/A	N/A	N/A	N/A	Not measured (islets used for perifusion studies)				41.4 ± 1.5 / 44.0 ± 1.8 (Hyperglycemic Clamp)	16.9 ± 0 / 16.9 ± 0	12.3 ± 0.2 / 12.1 ± 0.2 (Hyperglycemic Clamp)	N/A
7a (males) standard washout (Fig. 4A-G)	Gender comparison of Cd effect	m	12/10	2/1	1 mM	Regular/ 42% fat	40.74 ± 3.93	44.93 ± 6.26	47893 ± 3411	49779 ± 3492	Not measured (islets used for *ex vivo* GSIS)				45.1 ± 1.1 / 45.3 ± 0.7	17.8 ± 0 / 17.9 ± 0.1	19.1 ± 0.2 / 19.1 ± 0.1	N/A
7b (females) GSIS standard washout (Fig. 4-G)	Gender comparison of Cd effect	f	10/10	1/1			44.33 ± 7.70	30.61 ± 4.54	**52458 ± 2734***	**40767 ± 3849***	Measured at later time point (see 6b)				40.2 ± 2.9 / 42.3 ± 1.6	17.9 ± 0.1 / 18.0 ± 0.1	18.7 ± 0.2 / 19.2 ± 0.3	33.5 ± 0.9 / 33.8 ± 0.5
7b (females) prolonged washout (Fig. 4H, Suppl. Fig. 5)	Effect of prolonged washout in females	f					62.05 ± 6.43	52.05 ± 6.10	43544 ± 3704	42745 ± 4865	33.65 ± 15.14	119.28 ± 13.13	22337 ± 2293	23171 ± 2216	40.1 ± 3.5 / 44.7 ± 1.6	17.9 ± 0.1 / 18.0 ± 0.1	31.8 ± 1.1 / 31.7 ± 1.1	33.5 ± 0.9 / 33.8 ± 0.5

682

683 N/A = not applicable, BDL=below detectable limit.

Table 2: Linear regression analysis between insulin AUC (dependent variable), islet Cd content, islet Zn content and age (independent variable) in males alone (n=33), females alone (n=29) and combined male and female mice (n=62). *p<0.05, ***p<0.001.

		Model 1				Model 2			
Gender	**Predictor**	**Parameter Estimate**	**LCL Mean**	**UCL Mean**	**Pr > |t|**	**Parameter Estimate**	**LCL Mean**	**UCL Mean**	**Pr > |t|**
Males and females	**Gender**	5.65	-8.48	19.79	0.435	-17.36	-33.43	-1.29	0.039*
	Islet Cd	-0.15	-0.28	-0.02	0.028*	-0.09	-0.2	0.03	0.138
	Islet Zn	0.0005	$-12X10^{-5}$	0.001	0.115	0.0004	$-21X10^{-5}$	0.0009	0.217
	Age	-	-	-	-	1.36	0.75	1.98	<0.001***
Males	**Islet Cd**	-0.27	-0.48	-0.06	0.018*	-0.19	-0.37	-0.02	0.042*
	Islet Zn	0.0009	$-5 X 10^{-6}$	0.002	0.061	0.0007	$18X10^{-7}$	0.001	0.059
	Age	-	-	-	-	1.38	0.70	2.07	<0.001***
Females	**Islet Cd**	-0.04	-0.16	0.09	0.588	-0.02	-0.16	0.13	0.844
	Islet Zn	$-3X10^{-4}$	-0.001	0.0006	0.538	$-44X10^{-5}$	-0.002	0.0006	0.435
	Age	-	-	-	-	0.68	-1.85	3.2	0.604

LCL: lower control limits, UCL: upper control limits, Pr > |t|: t-distribution two-tailed p-value.

688 **Supplemental Figures**

689 Suppl. Fig. 1: (A) Glucose tolerance test and corresponding (B) area under the curve

690 (AUC) and (C) fasting body weight in mice exposed to either V (n=3) or 1mM $CdCl_2$ (n=5)

691 in drinking water for 12 months. Data are expressed as mean ± SEM.

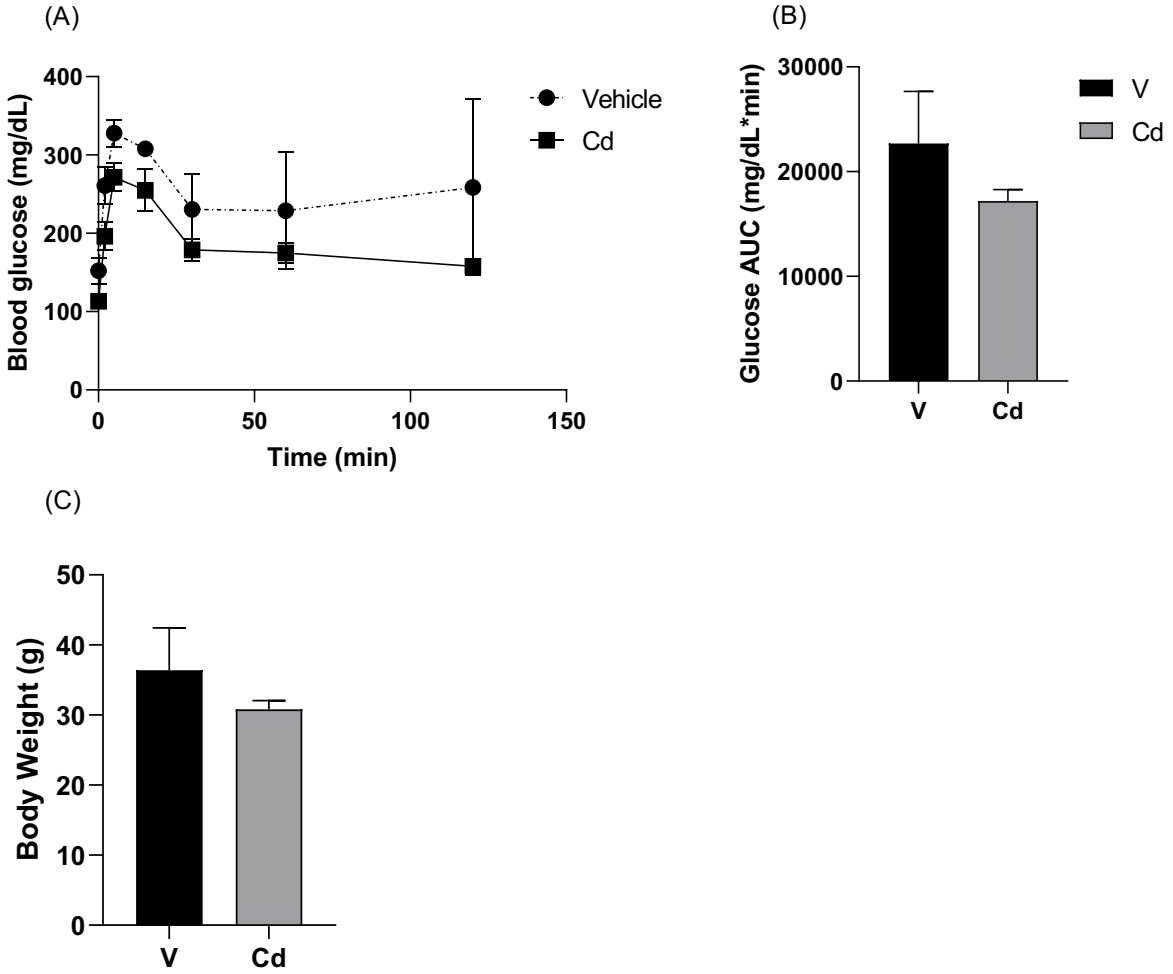

692

693

694 Suppl. Fig. 2**:** Rate of non-radioactive, rare Zn isotope, ^{67}Zn uptake as a proxy for Zn

695 turnover in MIN6 cells following exposure to either V or 0.5μM $CdCl_2$ for 48 hours (n=2).

696 Data are expressed as mean ± SEM.

697

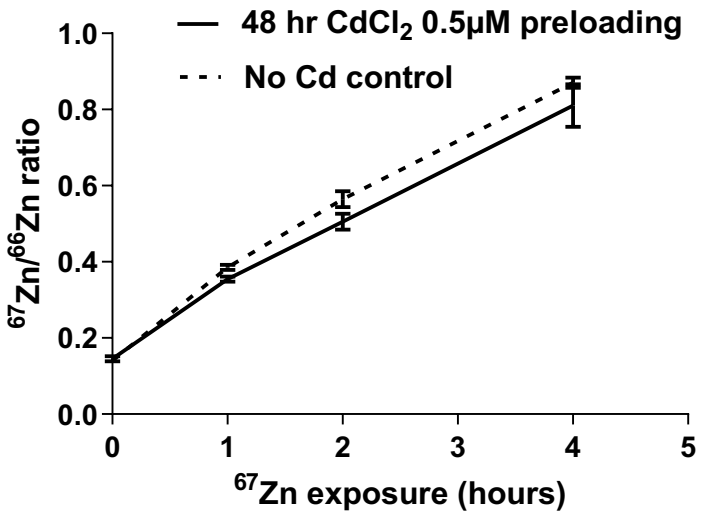

698

699

700 Suppl. Fig 3: (A) Blood glucose, (B) plasma insulin, (C) AUC glucose, (D) AUC insulin
701 and (E) fasting body weight during *in vivo* GSIS in male mice exposed to either V (n=9)
702 or 1mM $CdCl_2$ (n=10) for 19 weeks (Table 1, Cohort #4). GSIS was performed at the end
703 of the Cd exposure phase and prior to the commencement of the washout phase. Data
704 are expressed as mean ± SEM. *$p<0.05$.

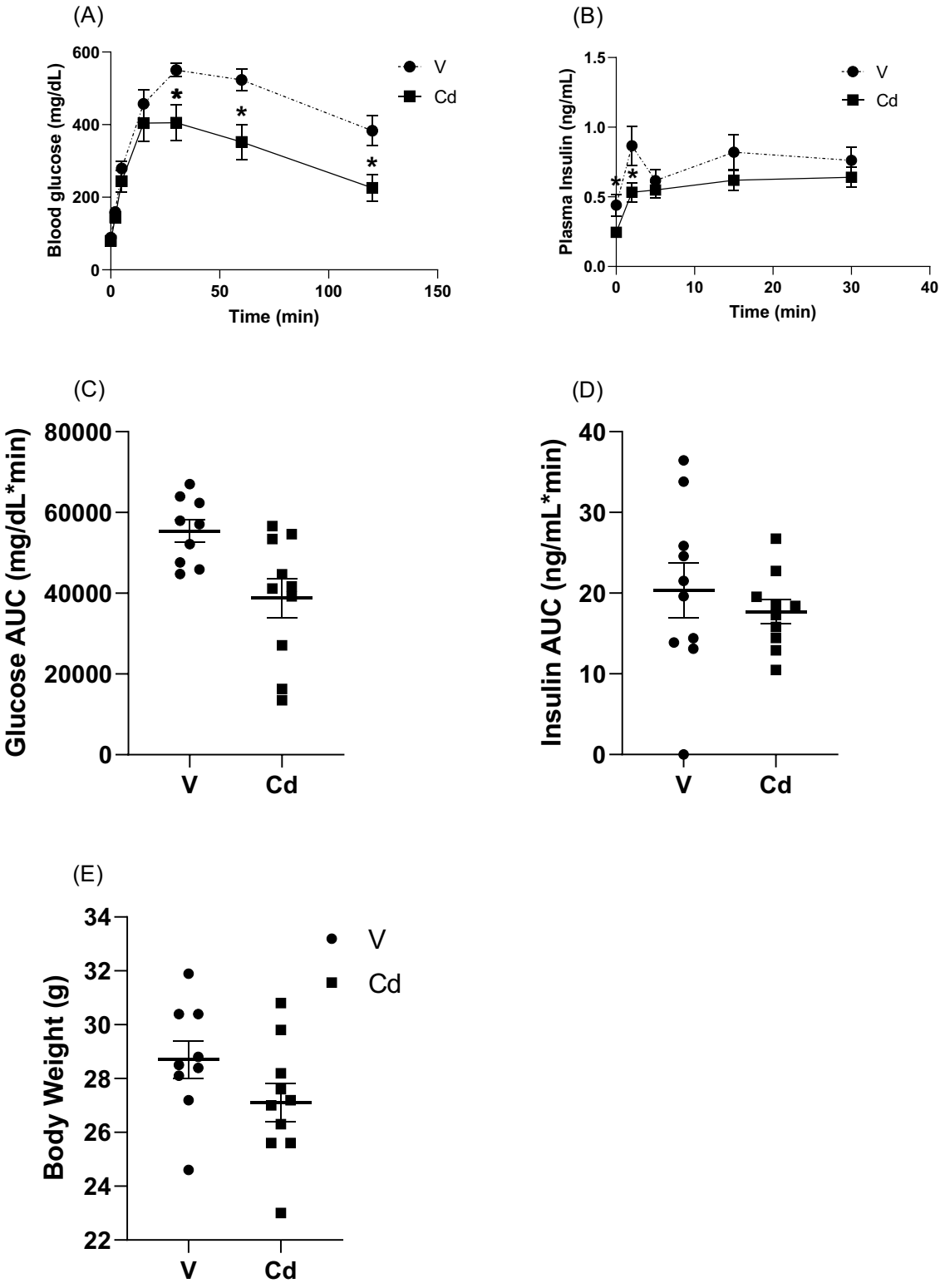
(A)
Blood glucose (mg/dL)
600
400
200
0
0
50
100
150
Time (min)
V
Cd
*
*
*
(B)
Plasma Insulin (ng/mL)
1.5
1.0
0.5
0.0
0
10
20
30
40
Time (min)
V
Cd
*
*
(C)
Glucose AUC (mg/dL*min)
80000
60000
40000
20000
0
V
Cd
(D)
Insulin AUC (ng/mL*min)
40
30
20
10
0
V
Cd
(E)
Body Weight (g)
34
32
30
28
26
24
22
V
Cd
V
Cd

705

706

707 Suppl. Fig 4: (A) Blood glucose, (B) plasma insulin, (C) AUC glucose, (D) AUC insulin
708 and (E) fasting body weight during *in vivo* GSIS in male mice exposed to either V (n=6)
709 or 1mM $CdCl_2$ (n=6) for 19 weeks followed by 28.9 weeks washout phase (table 1, Coort
710 #3). Mice were given HFD at both the Cd exposure and washout phases. V-HFD, V-
711 exposed group given HFD; Cd-HFD, Cd-exposed group given HFD. Data are expressed
712 as mean ± SEM. **$p<0.01$.

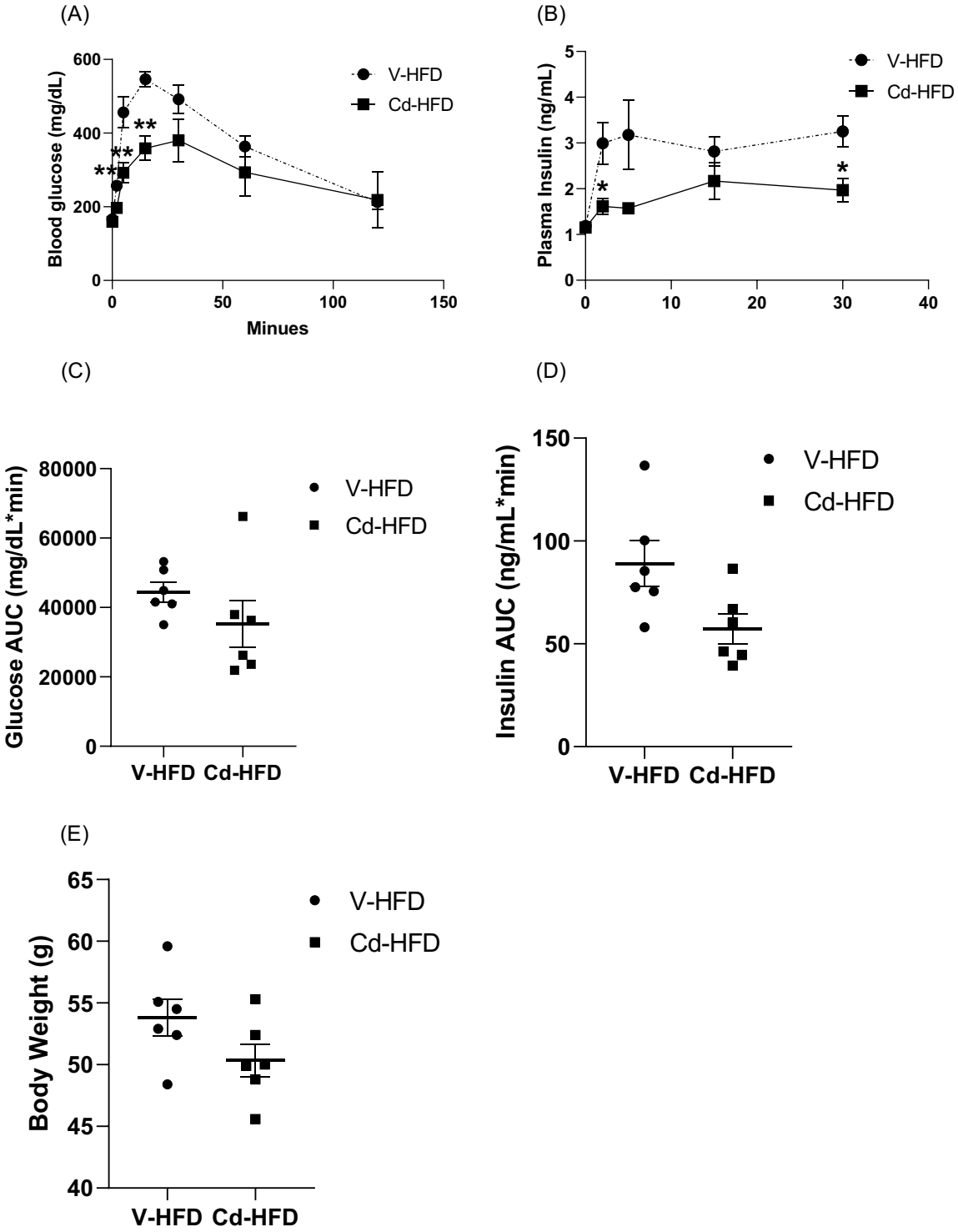
(A)
Blood glucose (mg/dL)
Minues
V-HFD
Cd-HFD
**
**
**
(B)
Plasma Insulin (ng/mL)
V-HFD
Cd-HFD
*
*
(C)
Glucose AUC (mg/dL*min)
V-HFD
Cd-HFD
(D)
Insulin AUC (ng/mL*min)
V-HFD
Cd-HFD
(E)
Body Weight (g)
V-HFD
Cd-HFD

713

714

715

716 Suppl. Fig 5: (A) Blood glucose, (B) plasma insulin, (C) AUC glucose, (D) AUC insulin
717 and (E) fasting body weight during *in vivo* GSIS in female mice exposed to either V (n=6)
718 or 1mM $CdCl_2$ (n=6) for 18 weeks followed by washout phase for 34 weeks with HFD
719 (Table 1, Cohort #7b). V-HFD, V-exposed followed by washout and HFD; Cd-HFD, Cd-
720 exposed followed by washout and HFD. Data are expressed as mean ± SEM.

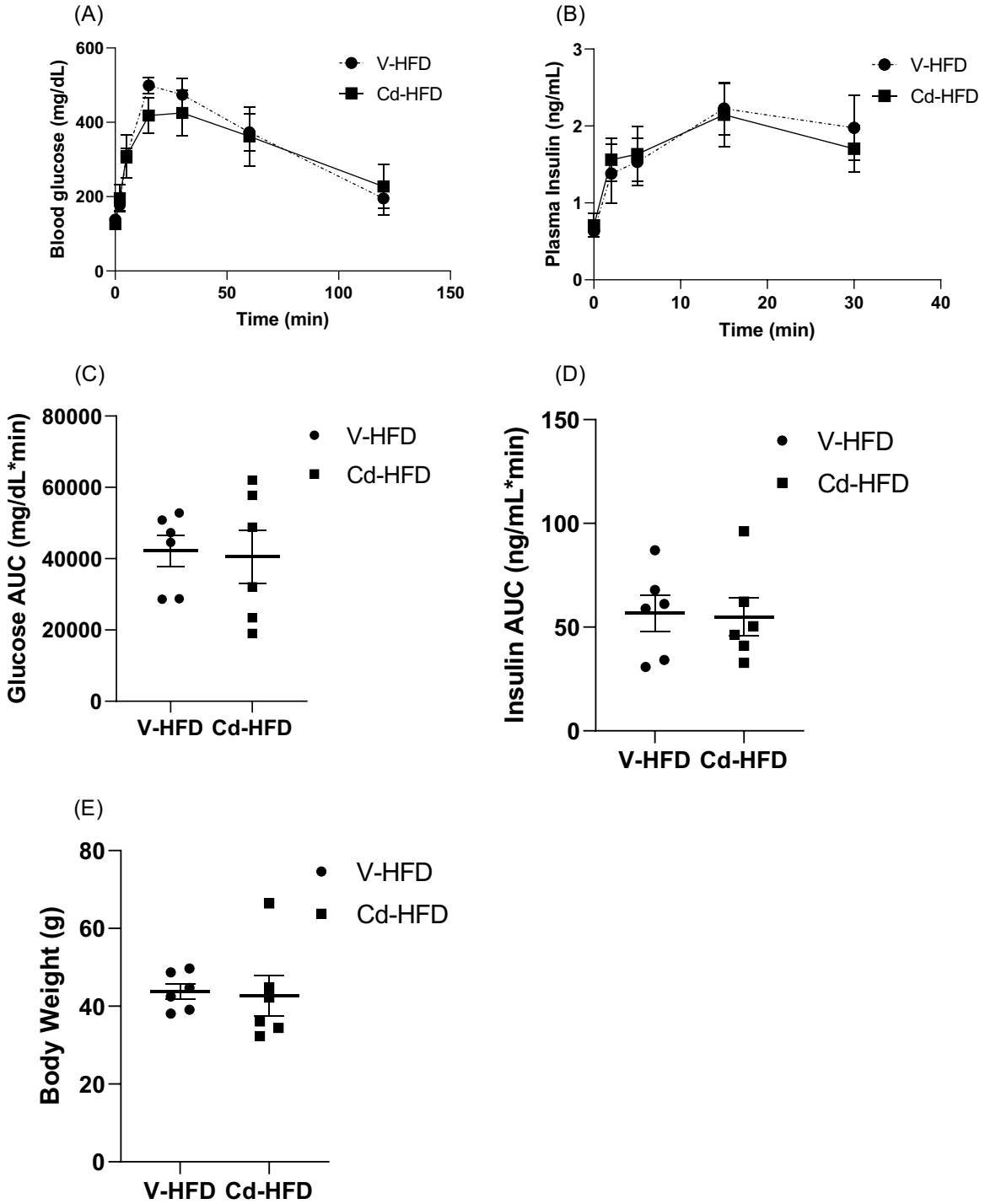
(A)
Blood glucose (mg/dL)
600
400
200
0
0
50
100
150
Time (min)
V-HFD
Cd-HFD
(B)
Plasma Insulin (ng/mL)
3
2
1
0
0
10
20
30
40
Time (min)
V-HFD
Cd-HFD
(C)
Glucose AUC (mg/dL*min)
80000
60000
40000
20000
0
V-HFD Cd-HFD
V-HFD
Cd-HFD
(D)
Insulin AUC (ng/mL*min)
150
100
50
0
V-HFD Cd-HFD
V-HFD
Cd-HFD
(E)
Body Weight (g)
80
60
40
20
0
V-HFD Cd-HFD
V-HFD
Cd-HFD

721

722

723 Suppl. Fig 6: (A) Blood glucose, (B) plasma insulin, (C) AUC glucose, (D) AUC insulin
724 and (E) fasting body weight during *in vivo* GSIS in female mice exposed to either V (n=7)
725 or 1mM $CdCl_2$ (n=8) for 18 weeks followed by 36 weeks washout phase (without Cd)
726 (Table 1, Cohort #4). Mice were given HFD at both the Cd exposure and washout phases.
727 V-HFD, V-exposed group given HFD; Cd-HFD, Cd-exposed group given HFD. Data are
728 expressed as mean ± SEM. *$p<0.05$.

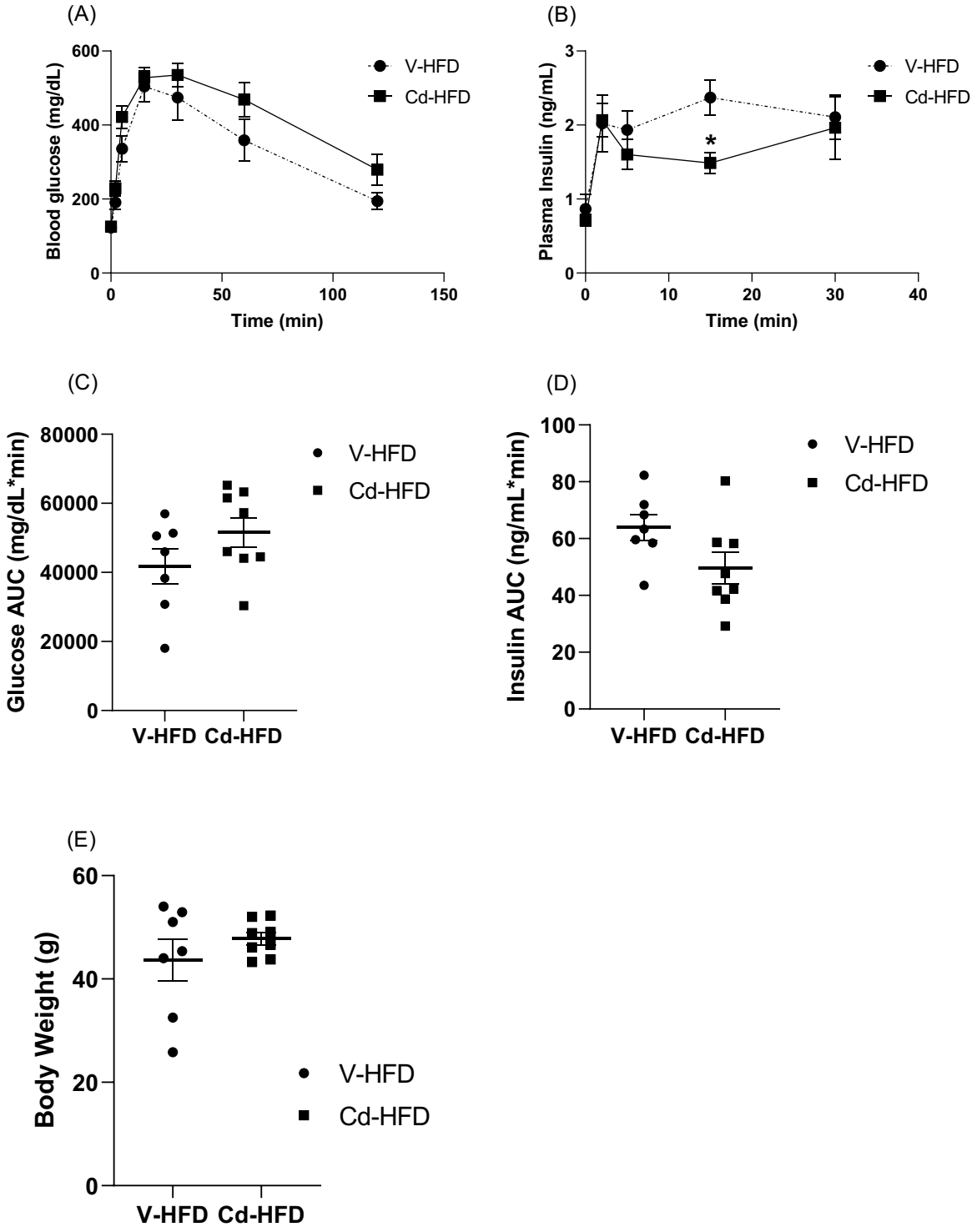
(A)
Blood glucose (mg/dL)
600
400
200
0
0
50
100
150
Time (min)
V-HFD
Cd-HFD
(B)
Plasma Insulin (ng/mL)
3
2
1
0
0
10
20
30
40
Time (min)
*
V-HFD
Cd-HFD
(C)
Glucose AUC (mg/dL*min)
80000
60000
40000
20000
0
V-HFD Cd-HFD
V-HFD
Cd-HFD
(D)
Insulin AUC (ng/mL*min)
100
80
60
40
20
0
V-HFD Cd-HFD
V-HFD
Cd-HFD
(E)
Body Weight (g)
60
40
20
0
V-HFD Cd-HFD
V-HFD
Cd-HFD

729

730

731 **Supplemental Table**

732 Suppl. Table 1: Serum Clinical Chemistry from male mice that were treated with either V
733 (n=9) or 1mM $CdCl_2$ (n=10) for 18 weeks followed by 26 weeks HFD thereafter. V-HFD,
734 V-exposed followed by washout with HFD mice; Cd-HFD, Cd-exposed followed by
735 washout with HFD mice. Data are expressed as mean ± SEM. *p<0.05.

Analyte	V-HFD	Cd-HFD
ALP (U/L)	105.4 ± 11.5	105.1 ± 11.6
AST (U/L)	503.8 ± 90.4	522.2 ± 86.4
ALT (U/L)	611.7 ± 115.8	678.3 ± 158.1
Creatine kinase (U/L)	793.2 ± 504.9	349.7 ± 84.8
GGT (U/L)	0 ± 0	0 ± 0
Albumin (g/dL)	2.5 ± 0.1	2.6 ± 0.1
Total Bilirubin (mg/dL)	0.14 ± 0.02	0.15 ± 0.02
Total Protein (g/dL)	5.2 ± 0.2	5.4 ± 0.2
Globulin (g/dL)	2.7 ± 0.1	2.8 ± 0.1
Bilirubin – Conjugated (mg/dL)	0.06 ± 0.02	0.05 ± 0.02
BUN (mg/dL)	16.2 ± 2.0	16.2 ± 1.1
Creatinine (mg/dL)	0.10 ± 0.03	0.16 ± 0.05
Cholesterol (mg/dL)	314.8 ± 22.7	305.0 ± 20.0
Glucose (mg/dL)	376.3 ± 15.5	412.3 ± 27.3
Calcium (mg/dL)	8.5 ± 0.2	8.8 ± 0.3
Phosphorus (mg/dL)	7.4 ± 0.6	8.5 ± 0.7
Bicarbonate TCO_2 (mM)	17.3 ± 0.7	17.1 ± 1.6
Chloride (mM)	113.1 ± 1.3	108.3 ± 1.3*
Potassium (mM)	6.1 ± 0.5	6.2 ± 0.7
ALB/GLOB ratio	0.9 ± 0.03	0.9 ± 0.03
Sodium (mM)	150.6 ± 0.9	148.4 ± 1.4
BUN/Creatinine ratio	92.2 ± 27.8	58.3 ± 18.0
Bilirubin – Unconjugated (mg/dL)	0.09 ± 0.03	0.12 ± 0.03
Na/K ratio	26.0 ± 2.4	26.0 ± 2.6
Triglycerides (mg/dL)	67.0 ± 3.7	57.6 ± 4.9
C-reactive peptide (ng/ml)	15234.1 ± 815.1	14033.4 ± 574.7

736

737 Suppl. Table 2A: Linear regression analysis between insulin AUC during GSIS
738 (dependent variable) and islet Cd content, islet Zn content, age and glucose AUC as
739 independent variables in males alone (n=33), females alone (n=29) and combined (n=62).

Gender	Predictor	Parameter Estimate	LCL Mean	UCL Mean	Pr > |t|
Males and females	**Gender**	-12.93	-30.22	4.37	0.149
	Islet Cd	-0.09	-0.20	0.03	0.137
	Islet Zn	0.0003	-24×10^{-5}	0.0009	0.257
	Age	1.27	0.65	1.90	<0.001
	AUC glucose	-37×10^{-5}	-92×10^{-5}	0.0002	0.196
Males	**Islet Cd**	-0.19	-0.37	-0.02	0.042
	Islet Zn	0.0007	-46×10^{-6}	0.001	0.077
	Age	1.33	0.61	2.06	0.001
	AUC glucose	-2×10^{-4}	-0.001	0.0006	0.634
Females	**Islet Cd**	-0.006	-0.15	0.14	0.931
	Islet Zn	-34×10^{-5}	-0.001	0.0007	0.529
	Age	0.49	-1.96	2.94	0.699
	AUC glucose	-56×10^{-5}	-0.001	0.0001	0.111

740 LCL: lower control limits, UCL: upper control limits, Pr > |t|: t-distribution two-tailed p-
741 value.
742

743 Suppl. Table 2B: Linear regression model between insulin AUC during GSIS (dependent
744 variable) and islet Cd content with successive addition of gender, islet Zn content, age
745 and AUC glucose as independent variables in males and females combined (n=62).
746

	Model											
	MODEL1				MODEL2				MODEL3			
	Parameter Estimate	LCLmean	UCLmean	Pr > |t|	Parameter Estimate	LCLmean	UCLmean	Pr > |t|	Parameter Estimate	LCLmean	UCLmean	Pr > |t|
Predictor												
Islet_Cd	-0.14	-0.26	-0.006	0.044	-0.14	-0.27	-0.007	0.043	-0.15	-0.28	-0.02	0.028
female	.	.	.	.	3.72	-10.40	17.84	0.607	5.65	-8.48	19.79	0.436
Islet_Zn	.	.	.	.	.	.	.	.	0.0005	-12E-5	0.001	0.115
Age	.	.	.	.	.	.	.	.	.	.	.	.
AUC_glucose	.	.	.	.	.	.	.	.	.	.	.	.

	Model							
	MODEL4				MODEL5			
	Parameter Estimate	LCLmean	UCLmean	Pr > |t|	Parameter Estimate	LCLmean	UCLmean	Pr > |t|
Predictor								
Islet_Cd	-0.09	-0.20	0.03	0.138	-0.09	-0.20	0.03	0.137
female	-17.36	-33.43	-1.29	0.039	-12.93	-30.22	4.37	0.149
Islet_Zn	0.0004	-21E-5	0.0009	0.217	0.0003	-24E-5	0.0009	0.257
Age	1.36	0.75	1.98	<.001	1.27	0.65	1.90	<.001
AUC_glucose	.	.	.	.	-37E-5	-92E-5	0.0002	0.196

747 LCL: lower control limits, UCL: upper control limits, Pr > $|t|$: t-distribution two-tailed p-
748 value.
749
750

751 Suppl. Table 2C: Linear regression model between insulin AUC during GSIS (dependent
752 variable) and islet Cd content with successive addition of islet Zn content, age, and AUC
753 glucose as independent variables in males (n=33).
754

	Model											
	MODEL1				MODEL2				MODEL3			
	Parameter Estimate	LCLmean	UCLmean	Pr > |t|	Parameter Estimate	LCLmean	UCLmean	Pr > |t|	Parameter Estimate	LCLmean	UCLmean	Pr > |t|
Predictor												
Islet_Cd	-0.27	-0.48	-0.06	0.018	-0.19	-0.37	-0.02	0.042	-0.19	-0.37	-0.02	0.042
Islet_Zn	0.0009	-5E-6	0.002	0.061	0.0007	18E-7	0.001	0.059	0.0007	-46E-6	0.001	0.077
Age	.	.	.	.	1.38	0.70	2.07	<.001	1.33	0.61	2.06	0.001
AUC_glucose	.	.	.	.	.	.	.	.	-2E-4	-0.001	0.0006	0.634

755 LCL: lower control limits, UCL: upper control limits, Pr > $|t|$: t-distribution two-tailed p-
756 value.
757
758

759 Suppl. Table 2D: Linear regression model between insulin AUC during GSIS (dependent
760 variable) and islet Cd content with successive addition of islet Zn content, age and AUC
761 glucose as independent variables in females (n=29).
762

	Model											
	MODEL1				MODEL2				MODEL3			
	Parameter Estimate	LCLmean	UCLmean	Pr > |t|	Parameter Estimate	LCLmean	UCLmean	Pr > |t|	Parameter Estimate	LCLmean	UCLmean	Pr > |t|
Predictor												
Islet_Cd	-0.04	-0.16	0.09	0.588	-0.02	-0.16	0.13	0.844	-0.006	-0.15	0.14	0.931
Islet_Zn	-3E-4	-0.001	0.0006	0.538	-44E-5	-0.002	0.0006	0.435	-34E-5	-0.001	0.0007	0.529
Age	.	.	.	.	0.68	-1.85	3.20	0.604	0.49	-1.96	2.94	0.699
AUC_glucose	.	.	.	.	.	.	.	.	-56E-5	-0.001	0.0001	0.111

763 LCL: lower control limits, UCL: upper control limits, Pr > $|t|$: t-distribution two-tailed p-
764 value.
765
766

767 Suppl. Table 3: Metal analysis for regular and high fat chow by ICP-MS normalized to

768 chow weight (n=3/group). Data are expressed as mean ± SEM.

Element	Regular chow, Envigo 7912 (ng element/g chow)	High fat chow, Envigo TD180240 (ng element/g chow)	High fat chow, Envigo TD88137 (ng element/ g chow)
^{7}Li	35.1 ± 4.9	0 ± 7.7	0 ± 1.0
^{55}Mn	42266.9 ± 7351.0	55231.8 ± 2919.6	46686.5 ± 463.6
^{57}Fe	112389.0 ± 4746.6	55883.5 ± 7653.1	755284.0 ± 25902.4
^{59}Co	344.5 ± 29.9	11.6 ± 1.2	12.4 ± 3.1
^{60}Ni	1302.8 ± 67.2	156.7 ± 46.0	76.7 ± 10.5
^{63}Cu	6676.0 ± 892.9	14361.6 ± 10018.0	6364.2 ± 988.5
^{66}Zn	37582.9 ± 681.1	7798.6 ± 773.6	7586.0 ± 982.1
^{75}As	87.1 ± 8.7	10.8 ± 1.0	11.4 ± 0.7
^{77}Se	219.4 ± 25.8	158.9 ± 21.3	196.7 ± 36.9
^{111}Cd	40.2 ± 4.9	33.8 ± 7.0	5.7 ± 0.4
^{182}W	63.2 ± 20.3	4.6 ± 0.9	2.3 ± 0.1
^{208}Pb	79.3 ± 41.5	23.9 ± 14.2	2.0 ± 0.8
^{202}Hg	1.2 ± 0.3	0.5 ± 0.1	0.1 ± 0.1

769

770

References

Afridi, H. I., T. G. Kazi, N. Kazi, M. K. Jamali, M. B. Arain, N. Jalbani, J. A. Baig and R. A. Sarfraz (2008). "Evaluation of status of toxic metals in biological samples of diabetes mellitus patients." Diabetes Res Clin Pract **80**(2): 280-288.

Antala, S. and R. E. Dempski (2012). "The human ZIP4 transporter has two distinct binding affinities and mediates transport of multiple transition metals." Biochemistry **51**(5): 963-973.

Arredondo, M., P. Munoz, C. V. Mura and M. T. Nunez (2003). "DMT1, a physiologically relevant apical Cu1+ transporter of intestinal cells." Am J Physiol Cell Physiol **284**(6): C1525-1530.

Ayala, J. E., V. T. Samuel, G. J. Morton, S. Obici, C. M. Croniger, G. I. Shulman, D. H. Wasserman, O. P. McGuinness and N. I. H. M. M. P. C. Consortium (2010). "Standard operating procedures for describing and performing metabolic tests of glucose homeostasis in mice." Dis Model Mech **3**(9-10): 525-534.

Banerjee, M., P. Vats, A. S. Kushwah and N. Srivastava (2019). "Interaction of antioxidant gene variants and susceptibility to type 2 diabetes mellitus." Br J Biomed Sci **76**(4): 166-171.

Barregard, L., G. Bergstrom and B. Fagerberg (2013). "Cadmium exposure in relation to insulin production, insulin sensitivity and type 2 diabetes: a cross-sectional and prospective study in women." Environ Res **121**: 104-109.

Beck, R., M. Chandi, M. Kanke, M. Styblo and P. Sethupathy (2019). "Arsenic is more potent than cadmium or manganese in disrupting the INS-1 beta cell microRNA landscape." Arch Toxicol **93**(11): 3099-3109.

Bell, R. R., J. L. Early, V. K. Nonavinakere and Z. Mallory (1990). "Effect of cadmium on blood glucose level in the rat." Toxicol Lett **54**(2-3): 199-205.

Cai, Y., C. P. Kirschke and L. Huang (2018). "SLC30A family expression in the pancreatic islets of humans and mice: cellular localization in the beta-cells." J Mol Histol **49**(2): 133-145.

Chang, K. C., C. C. Hsu, S. H. Liu, C. C. Su, C. C. Yen, M. J. Lee, K. L. Chen, T. J. Ho, D. Z. Hung, C. C. Wu, T. H. Lu, Y. C. Su, Y. W. Chen and C. F. Huang (2013). "Cadmium induces apoptosis in pancreatic beta-cells through a mitochondria-dependent pathway: the role of oxidative stress-mediated c-Jun N-terminal kinase activation." PLoS One **8**(2): e54374.

Chimienti, F., A. Favier and M. Seve (2005). "ZnT-8, a pancreatic beta-cell-specific zinc transporter." Biometals **18**(4): 313-317.

Coffey, R. and M. D. Knutson (2017). "The plasma membrane metal-ion transporter ZIP14 contributes to nontransferrin-bound iron uptake by human beta-cells." Am J Physiol Cell Physiol **312**(2): C169-C175.

Dalmieda, J. and P. Kruse (2019). "Metal Cation Detection in Drinking Water." Sensors **19**(23): 5134-5178.

Dalton, T. P., L. He, B. Wang, M. L. Miller, L. Jin, K. F. Stringer, X. Chang, C. S. Baxter and D. W. Nebert (2005). "Identification of mouse SLC39A8 as the transporter responsible for cadmium-induced toxicity in the testis." Proc Natl Acad Sci U S A **102**(9): 3401-3406.

El-Muayed, M., M. R. Raja, X. Zhang, K. W. MacRenaris, S. Bhatt, X. Chen, M. Urbanek, T. V. O'Halloran and W. L. Lowe Jr (2012). "Accumulation of Cadmium in Insulin-producing beta-cells." Islets **4**(6): 405-416.

El Muayed, M., M. R. Raja, X. Zhang, K. W. MacRenaris, S. Bhatt, X. Chen, M. Urbanek, T. V. O'Halloran and W. L. Lowe, Jr. (2012). "Accumulation of cadmium in insulin-producing beta cells." Islets **4**(6): 405-416.

817 Elinder, C. G., B. Lind, T. Kjellstrom, L. Linnman and L. Friberg (1976). "Cadmium in kidney
818 cortex, liver, and pancreas from Swedish autopsies. Estimation of biological half time in kidney
819 cortex, considering calorie intake and smoking habits." Arch Environ Health **31**(6): 292-302.
820 Fernandez-Twinn, D. S., L. Hjort, B. Novakovic, S. E. Ozanne and R. Saffery (2019).
821 "Intrauterine programming of obesity and type 2 diabetes." Diabetologia **62**(10): 1789-1801.
822 Fitzgerald, R., A. Olsen, J. Nguyen, W. P. Wong, M. El-Muayed and J. Edwards (2020).
823 "Pancreatic Islets Accumulate Cadmium in a Rodent Model of Cadmium-Induced
824 Hyperglycemia." International Journal of Molecular Sciences **22**(1): 360.
825 Friberg, L. (1984). "Cadmium and the kidney." Environ Health Perspect **54**: 1-11.
826 Friedman, R. (2014). "Structural and computational insights into the versatility of cadmium
827 binding to proteins." Dalton Trans **43**(7): 2878-2887.
828 Garrick, M. D., K. G. Dolan, C. Horbinski, A. J. Ghio, D. Higgins, M. Porubcin, E. G. Moore, L.
829 N. Hainsworth, J. N. Umbreit, M. E. Conrad, L. Feng, A. Lis, J. A. Roth, S. Singleton and L. M.
830 Garrick (2003). "DMT1: a mammalian transporter for multiple metals." Biometals **16**(1): 41-54.
831 Girijashanker, K., L. He, M. Soleimani, J. M. Reed, H. Li, Z. Liu, B. Wang, T. P. Dalton and D.
832 W. Nebert (2008). "Slc39a14 gene encodes ZIP14, a metal/bicarbonate symporter: similarities to
833 the ZIP8 transporter." Mol Pharmacol **73**(5): 1413-1423.
834 Hansen, J. B., M. F. Tonnesen, A. N. Madsen, P. H. Hagedorn, J. Friberg, L. G. Grunnet, R. S.
835 Heller, A. O. Nielsen, J. Storling, L. Baeyens, L. Anker-Kitai, K. Qvortrup, L. Bouwens, S.
836 Efrat, M. Aalund, N. C. Andrews, N. Billestrup, A. E. Karlsen, B. Holst, F. Pociot and T.
837 Mandrup-Poulsen (2012). "Divalent metal transporter 1 regulates iron-mediated ROS and
838 pancreatic beta cell fate in response to cytokines." Cell Metab **16**(4): 449-461.
839 Himeno, S., T. Yanagiya and H. Fujishiro (2009). "The role of zinc transporters in cadmium and
840 manganese transport in mammalian cells." Biochimie **91**(10): 1218-1222.
841 Hong, H., Y. Xu, J. Xu, J. Zhang, Y. Xi, H. Pi, L. Yang, Z. Yu, Q. Wu, Z. Meng, W. S. Ruan, Y.
842 Ren, S. Xu, Y. Q. Lu and Z. Zhou (2021). "Cadmium exposure impairs pancreatic beta-cell
843 function and exaggerates diabetes by disrupting lipid metabolism." Environ Int **149**: 106406.
844 Huang, C. C., C. Y. Kuo, C. Y. Yang, J. M. Liu, R. J. Hsu, K. I. Lee, C. C. Su, C. C. Wu, C. T.
845 Lin, S. H. Liu and C. F. Huang (2019). "Cadmium exposure induces pancreatic beta-cell death
846 via a Ca(2+)-triggered JNK/CHOP-related apoptotic signaling pathway." Toxicology **425**:
847 152252.
848 Jarup, L. and A. Akesson (2009). "Current status of cadmium as an environmental health
849 problem." Toxicol Appl Pharmacol **238**(3): 201-208.
850 Jarup, L., A. Rogenfelt, C. G. Elinder, K. Nogawa and T. Kjellstrom (1983). "Biological half-
851 time of cadmium in the blood of workers after cessation of exposure." Scand J Work Environ
852 Health **9**(4): 327-331.
853 Jin, T., G. F. Nordberg and M. Nordberg (1986). "Uptake of cadmium in isolated kidney cells--
854 influence of binding form and in vivo pretreatment." J Appl Toxicol **6**(6): 397-400.
855 Jolly, Y. N., A. Islam and S. Akbar (2013). "Transfer of Metals from Soil to Vegetables and
856 Possible Health Risk Assessment." SpringerPlus **15**(1): 385-393.
857 Kambe, T., H. Narita, Y. Yamaguchi-Iwai, J. Hirose, T. Amano, N. Sugiura, R. Sasaki, K. Mori,
858 T. Iwanaga and M. Nagao (2002). "Cloning and characterization of a novel mammalian zinc
859 transporter, zinc transporter 5, abundantly expressed in pancreatic beta cells." J Biol Chem
860 **277**(21): 19049-19055.
861 Kolb, H. and S. Martin (2017). "Environmental/Lifestyle Factors in the Pathogenesis and
862 Prevention of Type 2 Diabetes." BMC Medicine **15**(1): 131-142.

863 Kuo, C. C., K. A. Moon, S. L. Wang, E. Silbergeld and A. Navas-Acien (2017). "The
864 Association of Arsenic Metabolism with Cancer, Cardiovascular Disease, and Diabetes: A
865 Systematic Review of the Epidemiological Evidence." Environ Health Perspect **125**(8): 087001.
866 Lawlor, N., J. George, M. Bolisetty, R. Kursawe, L. Sun, V. Sivakamasundari, I. Kycia, P.
867 Robson and M. L. Stitzel (2017). "Single-cell transcriptomes identify human islet cell signatures
868 and reveal cell-type-specific expression changes in type 2 diabetes." Genome Res **27**(2): 208-
869 222.
870 Lawson, R., W. Maret and C. Hogstrand (2017). "Expression of the ZIP/SLC39A transporters in
871 beta-cells: a systematic review and integration of multiple datasets." BMC Genomics **18**(1): 719.
872 Lemaire, K., F. Chimienti and F. Schuit (2012). "Zinc transporters and their role in the pancreatic
873 beta-cell." J Diabetes Investig **3**(3): 202-211.
874 Li, X., M. Li, J. Xu, X. Zhang, W. Xiao and Z. Zhang (2019). "Decreased Insulin Secretion but
875 Unchanged Glucose Homeostasis in Cadmium-Exposed Male C57BL/6 Mice." J Toxicol **2019**:
876 8121834.
877 Li, Y. Y., C. Douillet, M. Huang, R. Beck, S. J. Sumner and M. Styblo (2020). "Exposure to
878 inorganic arsenic and its methylated metabolites alters metabolomics profiles in INS-1 832/13
879 insulinoma cells and isolated pancreatic islets." Arch Toxicol **94**(6): 1955-1972.
880 Lortz, S., S. Schroter, V. Stuckemann, I. Mehmeti and S. Lenzen (2014). "Influence of cytokines
881 on Dmt1 iron transporter and ferritin expression in insulin-secreting cells." J Mol Endocrinol
882 **52**(3): 301-310.
883 Martin, E., C. Gonzalez-Horta, J. Rager, K. A. Bailey, B. Sanchez-Ramirez, L. Ballinas-
884 Casarrubias, M. C. Ishida, D. S. Gutierrez-Torres, R. Hernandez Ceron, D. Viniegra Morales, F.
885 A. Baeza Terrazas, R. J. Saunders, Z. Drobna, M. A. Mendez, J. B. Buse, D. Loomis, W. Jia, G.
886 G. Garcia-Vargas, L. M. Del Razo, M. Styblo and R. Fry (2015). "Metabolomic characteristics
887 of arsenic-associated diabetes in a prospective cohort in Chihuahua, Mexico." Toxicol Sci
888 **144**(2): 338-346.
889 Menke, A., E. Guallar and C. C. Cowie (2016). "Metals in Urine and Diabetes in U.S. Adults."
890 Diabetes **65**(1): 164-171.
891 Miyazaki, J., K. Araki, E. Yamato, H. Ikegami, T. Asano, Y. Shibasaki, Y. Oka and K.
892 Yamamura (1990). "Establishment of a pancreatic beta cell line that retains glucose-inducible
893 insulin secretion: special reference to expression of glucose transporter isoforms." Endocrinology
894 **127**(1): 126-132.
895 Mohanasundaram, D., C. Drogemuller, J. Brealey, C. F. Jessup, C. Milner, C. Murgia, C. J.
896 Lang, A. Milton, P. D. Zalewski, G. R. Russ and P. T. Coates (2011). "Ultrastructural analysis,
897 zinc transporters, glucose transporters and hormones expression in New world primate
898 (Callithrix jacchus) and human pancreatic islets." Gen Comp Endocrinol **174**(2): 71-79.
899 Moon, S. S. (2013). "Association of lead, mercury and cadmium with diabetes in the Korean
900 population: the Korea National Health and Nutrition Examination Survey (KNHANES) 2009-
901 2010." Diabet Med **30**(4): e143-148.
902 Nie, X., N. Wang, Y. Chen, C. Chen, B. Han, C. Zhu, Y. Chen, F. Xia, Z. Cang, M. Lu, Y.
903 Meng, B. Jiang, D. J. M and Y. Lu (2016). "Blood cadmium in Chinese adults and its
904 relationships with diabetes and obesity." Environ Sci Pollut Res Int **23**(18): 18714-18723.
905 Nordberg, G. F. (2004). "Cadmium and health in the 21st century--historical remarks and trends
906 for the future." Biometals **17**(5): 485-489.

907 Ohana, E., I. Sekler, T. Kaisman, N. Kahn, J. Cove, W. F. Silverman, A. Amsterdam and M.
908 Hershfinkel (2006). "Silencing of ZnT-1 expression enhances heavy metal influx and toxicity." J
909 Mol Med (Berl) **84**(9): 753-763.
910 Petersmann, A., D. Muller-Wieland, U. A. Muller, R. Landgraf, M. Nauck, G. Freckmann, L.
911 Heinemann and E. Schleicher (2019). "Definition, Classification and Diagnosis of Diabetes
912 Mellitus." Exp Clin Endocrinol Diabetes **127**(S 01): S1-S7.
913 Scherer, G. and H. Barkemeyer (1983). "Cadmium Concentrations in Tobacco and Tobacco
914 Smoke." Ecotoxicology and Environmental Safety **7**(1): 71-78.
915 Schilderman, P. A., E. J. Moonen, P. Kempkers and J. C. Kleinjans (1997). "Bioavailability of
916 soil-adsorbed cadmium in orally exposed male rats." Environ Health Perspect **105**(2): 234-238.
917 Schwartz, G. G., D. II'yasova and A. Ivanova (2003). "Urinary Cadmium, Impaired Fasting
918 Glucose and Diabetes in the NHANES III." Diabetes Care **26**(2): 468-470.
919 Tallkvist, J., C. L. Bowlus and B. Lonnerdal (2001). "DMT1 gene expression and cadmium
920 absorption in human absorptive enterocytes." Toxicol Lett **122**(2): 171-177.
921 Todd, J. N., S. Srinivasan and T. I. Pollin (2018). "Advances in the Genetics of Youth-Onset
922 Type 2 Diabetes." Curr Diab Rep **18**(8): 57.
923 Trevino, S., M. P. Waalkes, J. A. Flores Hernandez, B. A. Leon-Chavez, P. Aguilar-Alonso and
924 E. Brambila (2015). "Chronic cadmium exposure in rats produces pancreatic impairment and
925 insulin resistance in multiple peripheral tissues." Arch Biochem Biophys **583**: 27-35.
926 Wallia, A., N. B. Allen, S. Badon and M. El Muayed (2014). "Association between urinary
927 cadmium levels and prediabetes in the NHANES 2005-2010 population." Int J Hyg Environ
928 Health **217**(8): 854-860.
929 Winslow, J. W. W., K. H. Limesand and N. Zhao (2020). "The Functions of ZIP8, ZIP14, and
930 ZnT10 in the Regulation of Systemic Manganese Homeostasis." Int J Mol Sci **21**(9).
931 Wong, W. P., N. B. Allen, M. S. Meyers, E. O. Link, X. Zhang, K. W. MacRenaris and M. El
932 Muayed (2017). "Exploring the Association Between Demographics, SLC30A8 Genotype, and
933 Human Islet Content of Zinc, Cadmium, Copper, Iron, Manganese and Nickel." Sci Rep **7**(1):
934 473.
935 Wong, W. P. S., J. C. Wang, M. J. Schipma, X. Zhang, J. R. Edwards and M. El Muayed (2021).
936 "Cadmium-mediated pancreatic islet transcriptome changes in mice and cultured mouse islets."
937 Toxicol Appl Pharmacol **433**: 115756.
938